Overview of axion astrophysics and perspectives from future astronomical probes

Oscar Straniero

Italian National Institute of Astrophysics

Workshop “Axions across boundaries”, Galileo Galilei Institute, Arcetri, May 3, 2023 `

Talk overview: FAQs

I will try to answer these frequently asked questions:

- Just bounds or real detections?
- How accurate are the astrophysical constraints?
- Which areas in the parameter space (m_a, $g_{a\gamma}$, g_{ae}…) can be investigated?

Axions & Astrophysics

Immediate goal: the use of astronomical sources as natural laboratories to constrain axiom and axion-like-particles physics.

Future perspective: the use of axions/ALPs as new astronomical messengers.

- **Astronomical Axion Sources:**
  - Stars - from the Sun to supernova progenitors,
  - Compact remnants of stellar evolution (White Dwarfs and Neutron Stars)
  - Stellar explosions (supernovae)
  - Active galactic nuclei (AGNs, Quasars, Blazars….)
- **TOOLS:**
  - Models of these astronomical sources
  - Accurate measurements: photometry, spectroscopy, astrometry …….

Axions & Astrophysics: just bounds or real detections?

We have to distinguish between **direct** and **indirect** searches:

- **direct** → directly point to the detection of axions emitted by an astronomical source (the Sun, giant stars, Blazars). Usually, these studies use the conversion of axions into photons in an external magnetic field, natural or artificial.
- **indirect** → search for anomalies in the macroscopic properties of cosmic objects, such as luminosity, temperature, electromagnetic spectrum…, looking for modifications possibly induced by interactions among axions and standard particles (photons, electrons….) .

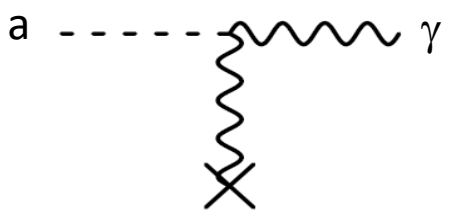

Since an anomalous macroscopic property may have alternative explanations, indirect searches provide bounds rather than real detections. These bounds, however, provide valuable hints for diret searches, because they restrict the search area.

Science cases

- The Sun → (weak) bounds, possible detection (axion telescopes)
- Globular cluster stars: RGB and HB stars → bounds
- Compact remnants of stellar evolution: WDs and NSs → bounds
- Supernova progenitors → bounds, possible detection (X-ray telescope)
- Core collapse Supernovae → bounds
- Extragalactic sources: Blazars → bounds, possible detection (X-ray spectra)
- Dark matter → bounds, possible detection (axion telescopes)
- ……

How to use stars as laboratories to probe new physics: a general strategy

- **The method is straightforward:**
  1. **identification of stellar properties much sensitive to the new physics ingredient,**
  2. **comparisons between theoretical predictions and astronomical observations.**
- To be competitive with laboratory experiments, the error budget should be reduced as much as possible.
- **The main issue is the evaluation of all the sources of errors, those affecting both the theoretical predictions and their observational counterparts.**
- The main risk is to underestimate the global error.

An example: Stars as laboratories, to probe new physics

- For instance, consider the energy balance:

$$\frac{dL}{dr} = (\epsilon_N + \epsilon_g - \epsilon_\nu) 4\pi r^2 \rho \quad \rightarrow \quad L = \int_0^R \frac{dL}{dr} dr$$

$\epsilon_N \rightarrow$ nuclear

$\epsilon_g = -T \frac{dS}{dt} \rightarrow$ gravity

$\epsilon_\nu \rightarrow$ thermal neutrinos

To be compared to:

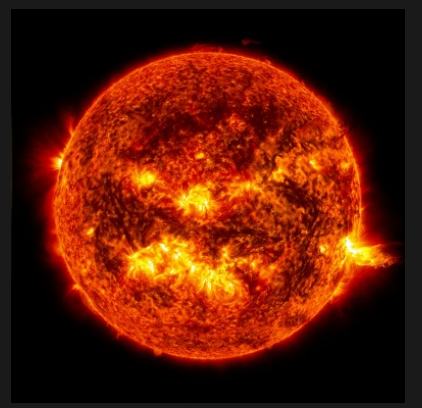

Hints of new physics or systematic errors ?

Suppose to find a discrepancy between *theoretical predictions* and *observations*. It may be due to either:

- Uncertainties in the theoretical recipe and/or in the observed luminosity
- **Missing physics!!!**

Some example of missing physics:

- **non-vanishing neutrino magnetic moment. It would enhance ϵ_ν**
- **non-standard energy sink (e.g., ALP production): $\epsilon_N + \epsilon_g - \epsilon_\nu - \epsilon_X$**
- **additional energy transport process as due scattering, absorption or decay of non-standard particles (e.g., massive ALPs).**

Hints for new physics or systematic errors ?

Some example of theoretical errors:

- **in general, uncertainties affecting $\epsilon_N, \epsilon_g, \epsilon_\nu$, e.g., unknown low-energy nuclear states may affect fusion cross sections and, in turn, ϵ_N.).**

Some example of observational errors:

- **systematic errors affecting photometry, parallaxes, light extinction …… all of them affecting L_{obs} .**

Hints for new physics or systematic errors ?

The conditions for being able to say, without doubt:

"I am seeing axions“

1. Be sure of having considered all the possible sources of uncertainty and that the global error is smaller than the discrepancy between theory and observation.

2. There are no alternative explanations.

keeping in mind these conditions, let me illustrate some of the current results

Constraining $g_{a\gamma}$ and g_{ae} with Globular Cluster stars

Globular Clusters

- **GCs are building blocks of any kind of galaxy.** They are found in giant spirals (such as the Milky Way or M31), ellipticals (M87) as well as in Dwarfs Spheroidals or irregular galaxies (e.g. Magellanic Clouds).
- **Hundreds of GCs populate the galactic halo and bulge**. They are old (~13 Gyr) and contain up to 10^7 stars gravitationally bound.
- Most of their stars are nearly coeval, even if there exists a growing amount of observational evidences showing that they **host multiple stellar populations**.
- GCs provide excellent laboratories to investigate new physics, because of:
  1. A large number of stars;
  2. Almost homogeneous stellar sample

Color Magnitude diagram and evolutionary phases

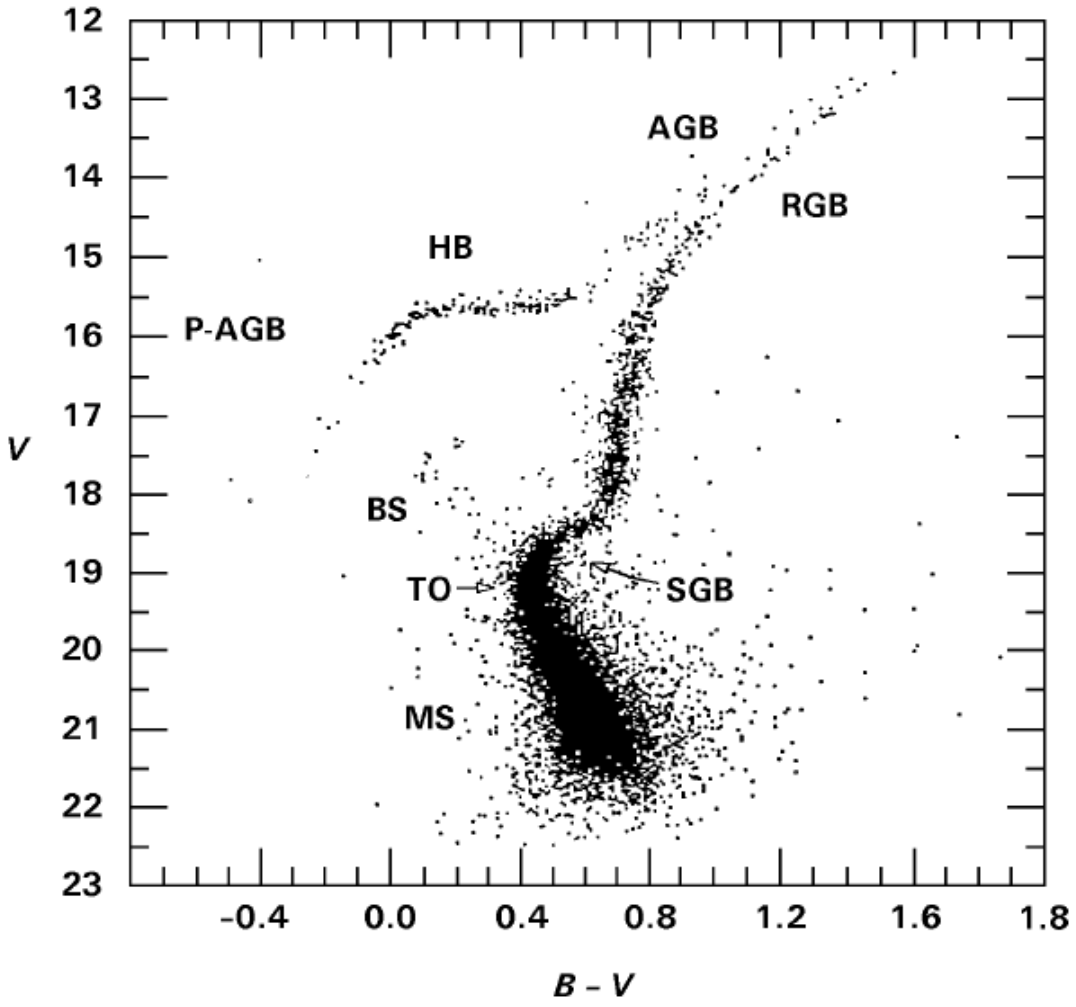

Main Sequence (MS): core-H burning, the longer evolutionary Phase.

Sub Giant Branch (SGB): Transient stars, between MS and RGB. H just exhausted in the center, external convection penetrates inward, first dredge up.

Red Giant Branch (RGB): An He-rich core, surrounded by an H-rich envelope. An H burning shell develops, the external layers expands, while the core contracts and electron degeneracy developes.

Horizontal Branch (HB): core-He burning stars. A convective envelope develops, surrounded by a semiconvective layer.

Asymptotic Giant Branch (AGB): degenerate CO core+He-rich mantel+H-rich envelope. Early-AGB, double shell burning, He and H, both active. Late-AGB. H-shell burning (most of the time) and recursive He-shell flashes (thermal pulses).

Galactic GC laboratory: observables & axions

Observable	ALPs production process
• Luminosity of the RGB tip	Bremsstrahlung
• RGB Luminosity Function	Bremsstrahlung
• Luminosity of the ZAHB	Bremsstrahlung
• *$R=N_{HB}/N_{RGB}$ ($R2=N_{AGB}/N_{HB}$)*	*Compton+Primakoff/Bremsstrahlung*
• *RR-Lyrae pulsation properties*	Bremsstrahlung

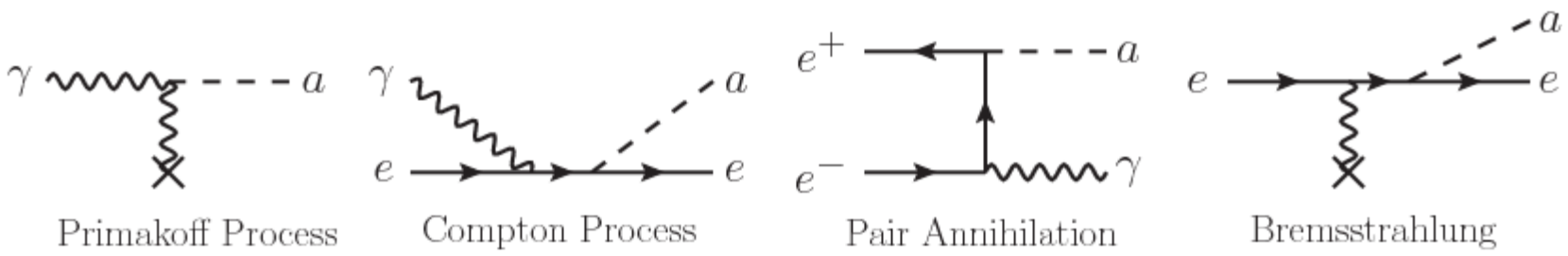

DATA requirements:

- Multiband observations (visible and infrared light) , to reconstruct the Spectral Energy Distribution (SED).
- Combination of high angular resolution observations from space, to resolve the most crowded central region, and large field-of-view observations (ground based telescopes), to increase the stellar sample.
- Astrometry may be used to clean the sample from field star contaminations and for distance determinations.

47 tuc seen by HST (right) and by a wider FOV ground based telescope (left).

MASS SEGREGATION: RGB stars are among the heaviest objects. They slow down and sink to the cluster's core.

Axions processes & rates

Raffelt & Dearborn 1987
Raffelt & Weiss 1995
Raffelt 1996
Nakawaga et al.1987, 1988
(revised by us)

Compton

$$\varepsilon_{\rm compton} = \theta_{\rm deg} 2.66 \times 10^{-48}\, g_{13}^2\, \frac{T^6}{\mu_e}\, {\rm erg\,g^{-1}\,s^{-1}}$$

Bremsstrahlung non degenerate (ND)

$$\varepsilon_{\rm BND} = 4.7 \times 10^{-25} g_{13}^2 T^{2.5}\, \frac{\rho}{\mu_e} \sum \frac{X_j}{A_j} \left[Z_j^2 \left(1 - \frac{5}{8}\frac{k_S^2}{m_e T}\right) + \frac{Z_j}{\sqrt{2}} \left(1 - \frac{5}{4}\frac{k_S^2}{m_e T}\right)\right] {\rm erg\,g^{-1}\,s^{-1}}$$

Bremsstrahlung Degenerate (D)

$$\varepsilon_{\rm BD} = 8.6\, F \times 10^{-33} g_{13}^2 T^4 \sum \frac{X_j Z_j^2}{A_j}$$

Weak coupling $\Gamma < 1$

$$\varepsilon = \left(\frac{1}{\varepsilon_{\rm D}} + \frac{1}{\varepsilon_{\rm ND}}\right)^{-1}$$

Primakoff ND & D

$$\begin{cases} \varepsilon_{\rm nd} = 7.1 \times 10^{-52}\, g_{10}^2 \left(\frac{T^7}{\rho}\right) y_1^2\, f(y_0, y_1)\,, \\ \varepsilon_{\rm ions} = 7.1 \times 10^{-52}\, g_{10}^2 \left(\frac{T^7}{\rho}\right) y_{\rm ions}^2\, f(y_0, y_{\rm ions})\,, \\ \varepsilon_{\rm el} = 4.7 \times 10^{-31}\, g_{10}^2\, R_{\rm deg} \left(\frac{T^4}{\mu_e}\right) f(y_0, y_{\rm TF})\,, \\ \varepsilon_{\rm deg} = \varepsilon_{\rm ions} + \varepsilon_{\rm el}\,, \\ \varepsilon_{\rm Tot} = (1-w)\varepsilon_{\rm nd} + w\,\varepsilon_{\rm deg}\,. \end{cases}$$

$$\varepsilon_{axi} = \varepsilon_{comp} + \varepsilon_{brem} + \varepsilon_{prim}$$

A single evolutionary track is made of a series of stellar models that start with a newborn proto-star and evolve its internal physical and chemical structure up to the final configuration (a compact white dwarf for GC stars).

$$\frac{dP}{dm_r} = -\frac{GM_r}{4\pi r^4}$$ ***Hydrostatic* equilibrium**

$$\frac{dr}{dm_r} = \frac{1}{4\pi r^2 \rho}$$ **Mass conservation**

$$\frac{dL_r}{dm_r} = \varepsilon_{nucl} - \varepsilon_{\nu} + \varepsilon_{grav}$$ **Energy conservation**

$$\frac{dT}{dm_r} = -\nabla \frac{GM_r}{4\pi r^4}\frac{T}{P}$$ **Energy transport**

$$\frac{dY_i}{dt} = \left(\frac{dY_i}{dt}\right)_{nuc} + \left(\frac{dY_i}{dt}\right)_{mix} \qquad i = 1,\ldots\ldots,N$$

Nuclear reactions + turbulent convection

4+N differential equations, in 4+N dependent variables:

- r (radius),
- L_r (luminosity),
- P (pressure),
- T (temperature),
- Y_i (chemical composition: abundances)

all depending on the lagrangian mass coordinate:

- $m_r = \int_0^r 4\pi\rho r^2 dr$

and the time: t

*Appropriate boundary conditions needed

1 stellar model contains about 1000 mesh points: m_r=(0,M)

1 evolutionary track contains up to 20000 stellar models: t = (0,13 Gyr)

$R=N_{HB}/N_{RGB}$ parameter

The number of stars observed in a given portion of the CM diagram is proportional to the time spent by a star in this region. ALPs ***electron coupling (Bremsstrahlung)*** affects N_{RGB}, while **photon coupling (Primakoff)** affects N_{HB} .

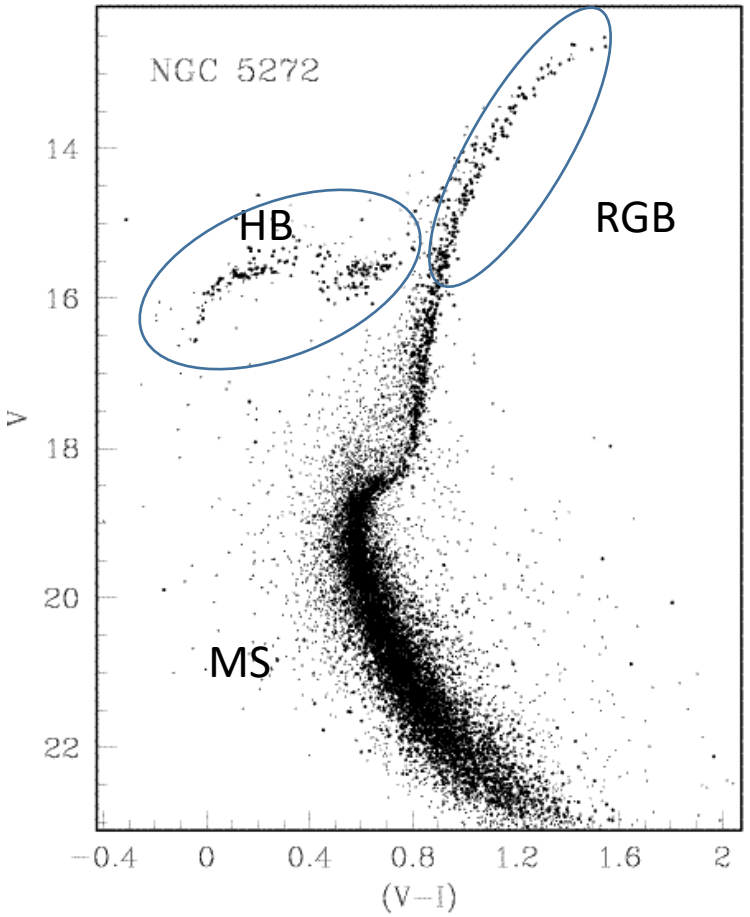

$$R = \frac{N_{HB}}{N_{RGB}}$$

- R does **not depend on metallicity, distance, light absorption and age**.
- R **depends on Y (!!)**

39 GCs (from the Salaris et al 2004 catalog)

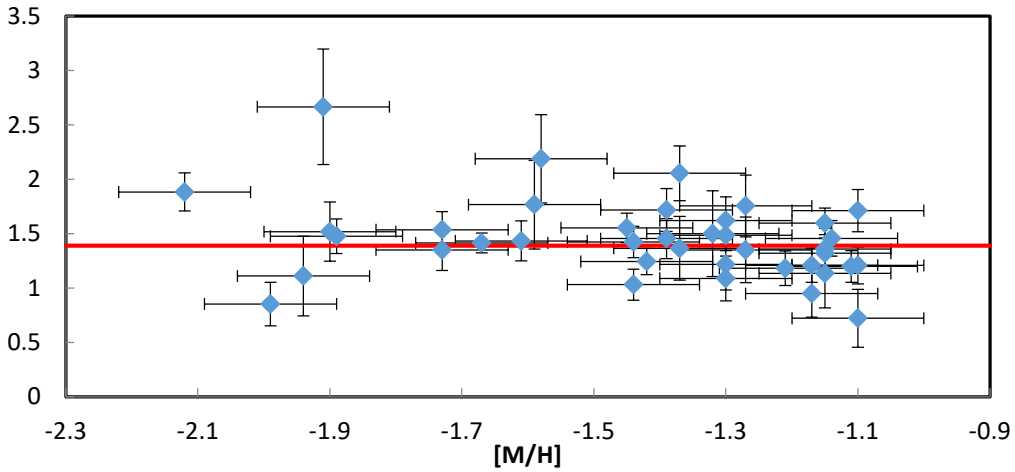

<R> = 1.39±0.03

Synthetic CM diagrams

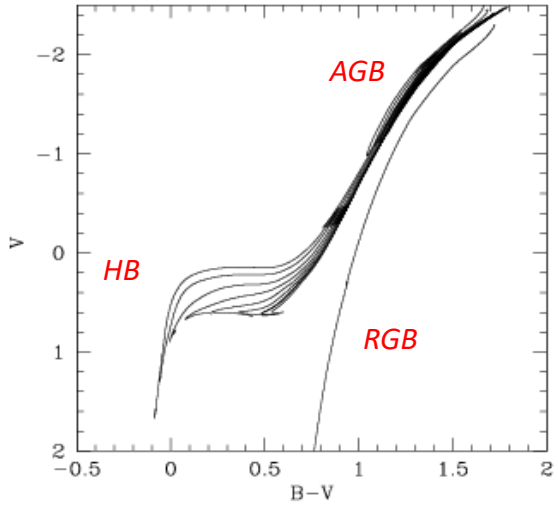

For each pair (Y, $g_{a\gamma}$) we calculate a set of evolutionary tracks: The total mass of the HB models is varied from 0.58 to 0.76, to account for the RGB mass loss causing the observed HB color spread.

Synthetic CM diagrams: 3 parameters: initial mass (Salpeter like distr. $\frac{dn}{dm} \propto m^{-\alpha}$), HB mass spectrum (gaussian), photometric errors (gaussian) .

$\sigma(M_{HB})=0.1\ M_{\odot}$
$\sigma(V)=0.01$ mag
$\sigma(B\text{-}V)=0.014$ mag

$N=3\times10^5$ $\sigma_{stat}(R)<1\%$
only 1000 synthetic stars plotted here.

Synthetic CM diagrams, with different $<M_{HB}>$

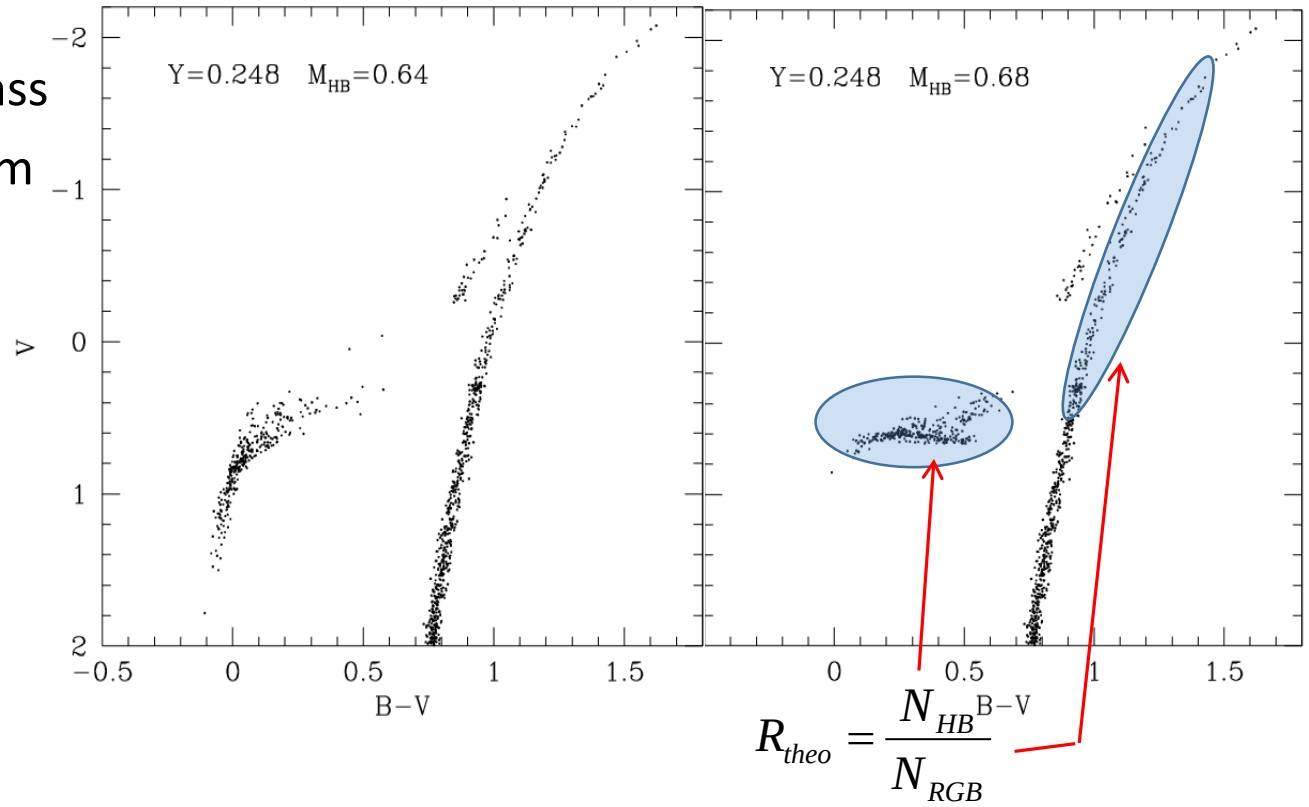

Multiple populations

Examples of simulations with 30% of He enhanced stars

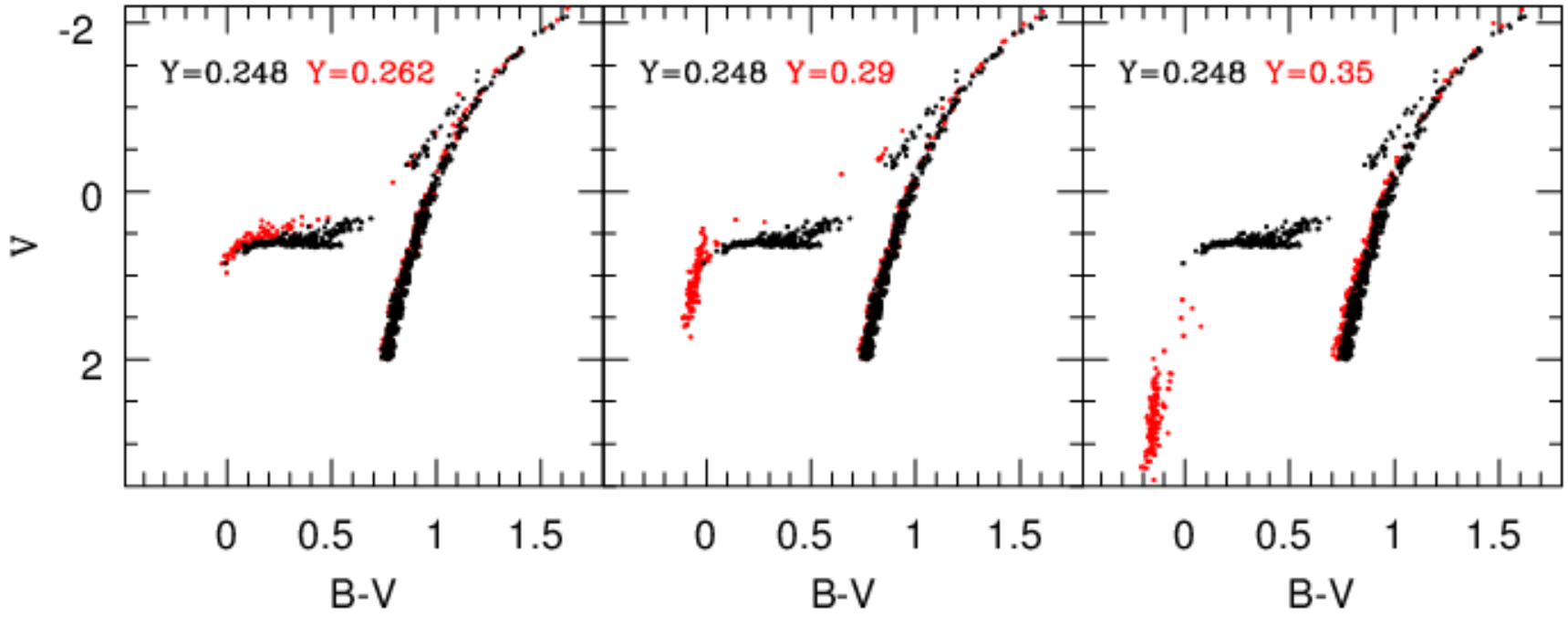

R=1.408 ***R=1.448*** ***R=1.548***

To be compared with single population ***R=1.408***

Clusters with blue HB tails not considered

Theory versus observations

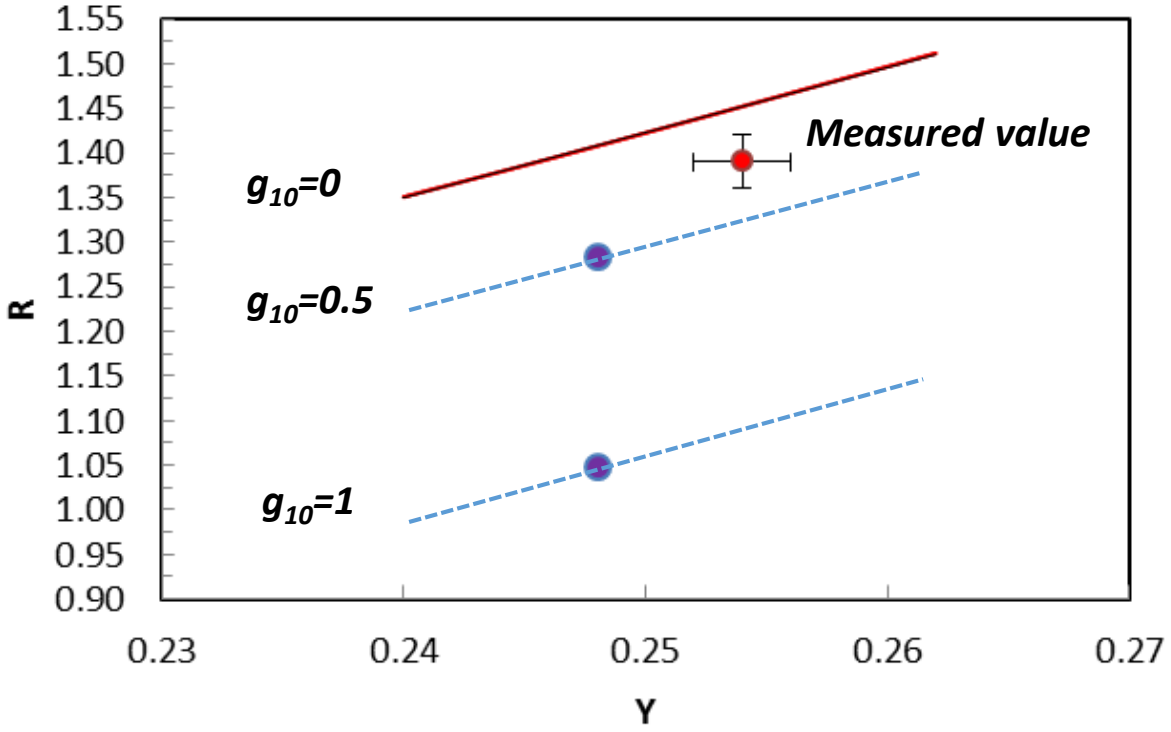

The larger the coupling the smaller the R parameter. However, a smaller R may be obtained by reducing the helium abundance (Y)

$$g_{\alpha\gamma} = a\delta^2 + b\delta$$

$$\delta = R_{g=0} - R = cY + f(r1, r2, r3) + d - R$$

$$a = 5.2706 \qquad b = 4.675$$

$$c = 7.3306 \qquad d = -0.409$$

Model prescriptions and error budget

Measured parameters

Parameter	uncertainty	Reference
R	1.39±0.03	Ayala et al. 2014
Y	0.255±0.005	Y_p+ΔY (Izotov et al. 2015, Aver et al. 2014)

Model Parameters: Nuclear reaction rates

Reaction	uncertainty	Reference
^{4}N(p,γ)^{15}O	10%	SF II , Adelberger et al. 2011 (LUNA 2005)
^{4}He(2α,γ)^{12}C	10%	Angulo et al. 1999 (NACRE), Fymbo 2005
^{12}C(α,γ)^{16}O	30%	Kunz et al. 2001 , Shurman et al. 2013 deBoer 2017

Treatment of convection (HB):

Induced overshoot (He -> C,O) + Semiconvection
(see Straniero et al 2003, ApJ 583, 878)

Plasma neutrinos (RGB):

Esposito et al. 2003, Nucl. Phys. B 658, 217
Haft et al. 1994 ApJ. 425, 222
Itoh et al. 1996, ApJ 470, 1015 .

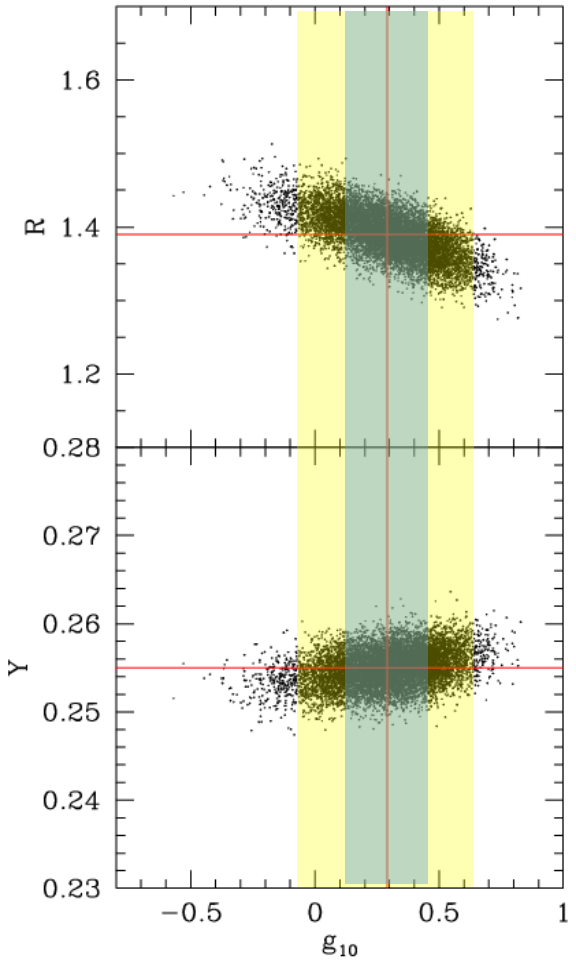

MC 5 PARAMETERS

Nuclear reaction rates:

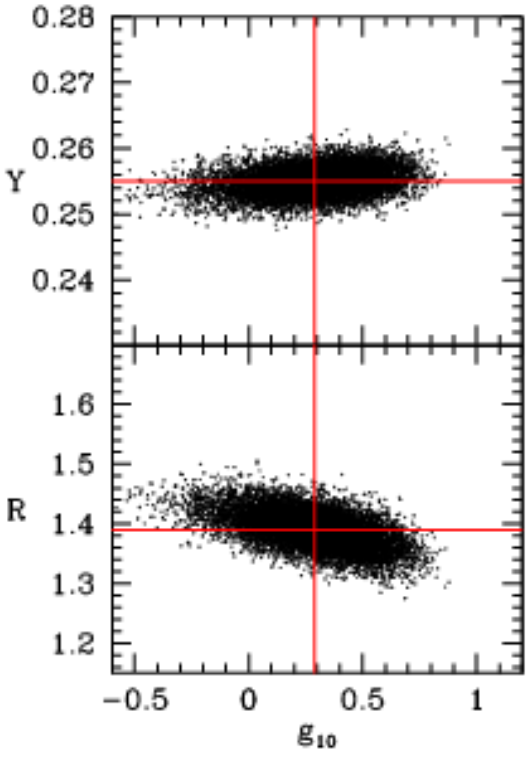

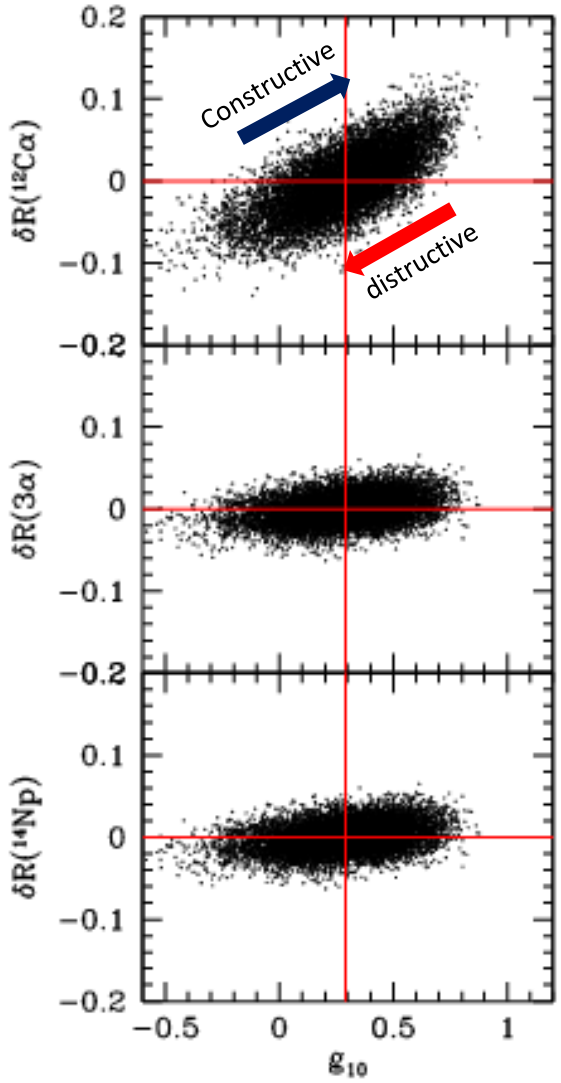

Strong influence of the $^{12}C(\alpha,\gamma)^{16}O$ rate.
At 300 keV (Gamow's peak), the cross section is dominated by ground state captures through two subthreshold resonances (J^{π} =1$^-$ and 2$^+$). The current estimation of S(E) is done by means of R-matrix calculations (deBoer+ 2017), combining direct and indirect measurements. Interferences with higher E states and direct captures can substantially affect the S(E).

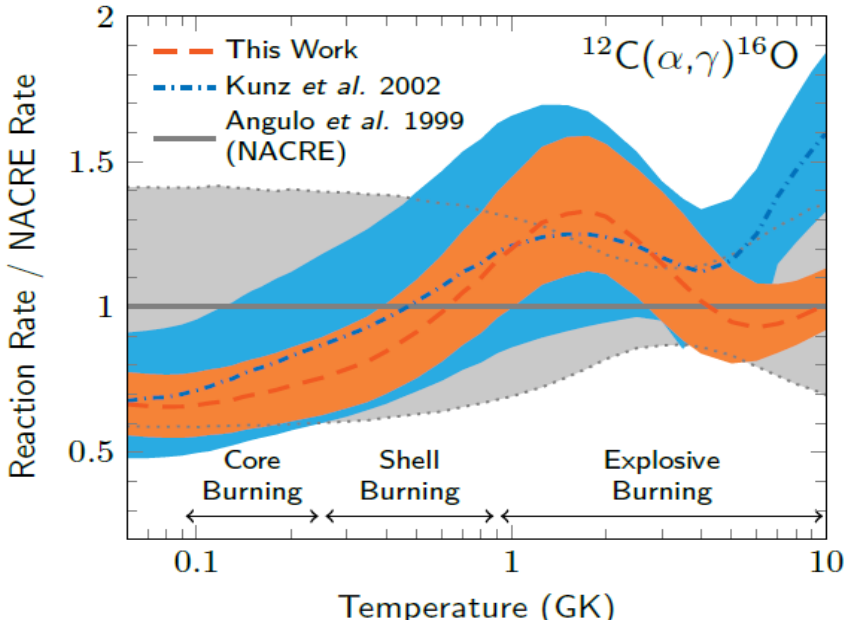

Summary:

- By means of synthetic CM diagrams, we have calculated the relation between $g_{\alpha\gamma}$ and 5 parameters, namely $R=N_{HB}/N_{RGB}$, Y, and the 3 more relevant nuclear reaction rates affecting the HB and the RGB timescale.
- By combining the uncertainties on this 5 parameters we find:

$$g_{a\gamma}=0.29\pm0.18\ (x10^{-10}\ GeV^{-1})$$

and a axion-photon coupling upper bound (95% CL):

$$g_{a\gamma}< 0.65\ (x10^{-10}\ GeV^{-1})$$

Combined Likelihood: axion-electron coupling would affect the N_{RGB} (Bremsstrahlung) and, to a less extent, N_{HB} (Compton).

So, varying the triplet g_{10},g_{13},Y:

$$L(g13, g10) = \exp\left[-\frac{(R_{th} - R_{obs})^2}{\sigma_{obs}^2 + \sigma_Y^2 + \sigma_{th}^2} \right]$$

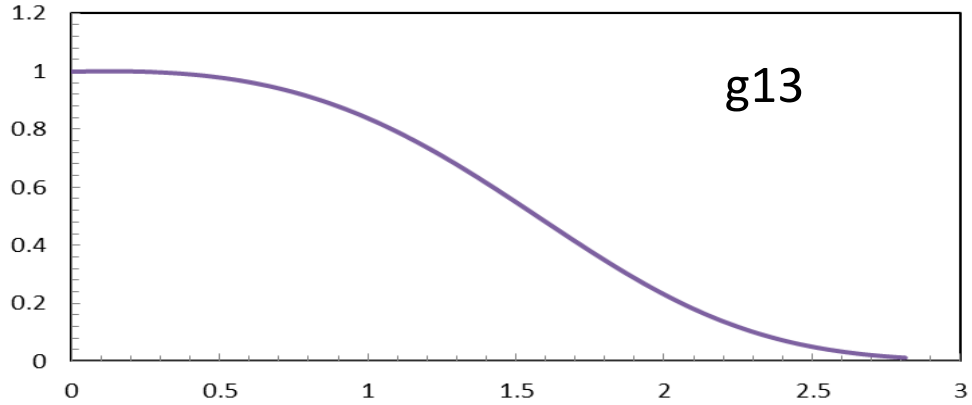

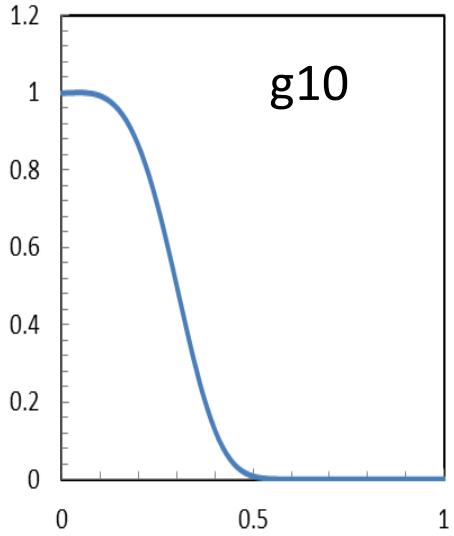

Error budget:

$\sigma(R_{obs})$	±0.03
$\sigma(Y)$	±0.015
$\sigma(R_{th})$	±0.04

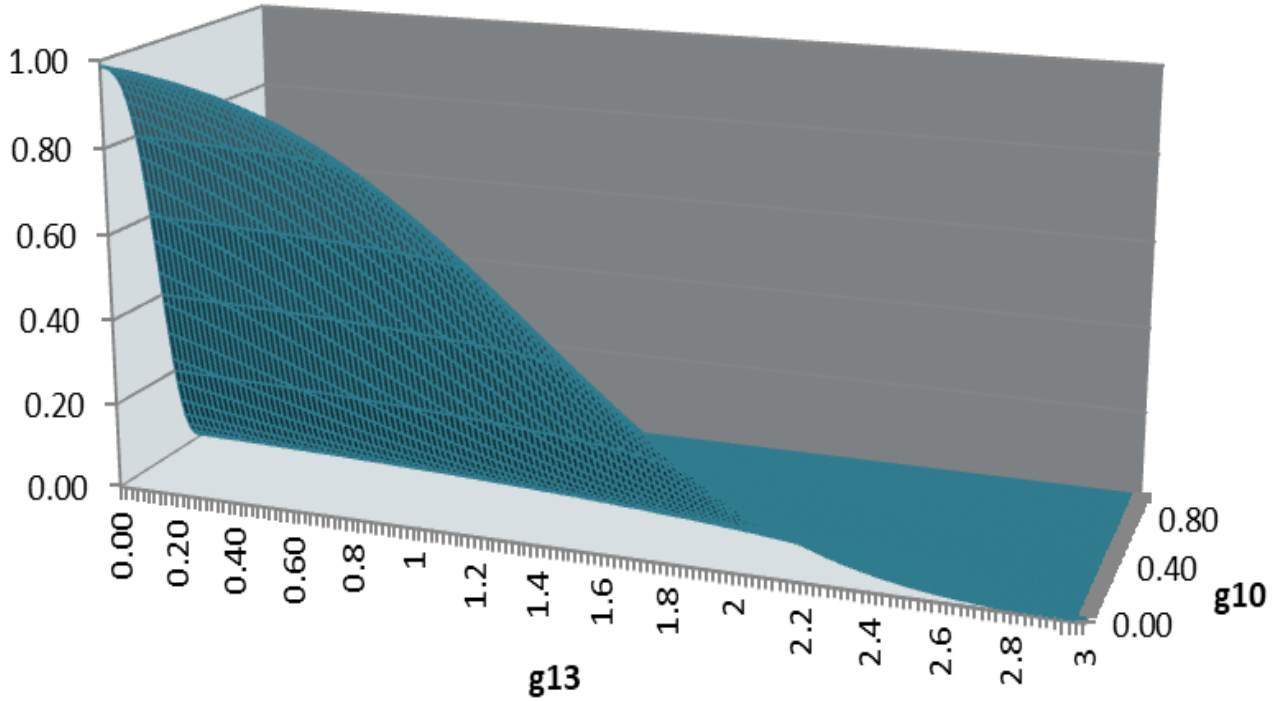

Upper bounds 95% C.L. ($m_a \leq 1$ keV) $g_{a\gamma} < 6 \times 10^{-11}$ GeV^{-1} and $g_{ae} < 2.6 \times 10^{-13}$ *(Ayala+ 2014 , Straniero+ 2017).*

For more massive ALPs, ***photon coalescence and ALP trapping*** *play relevant roles: Carenza+ 2018, Luente+. 2022.*

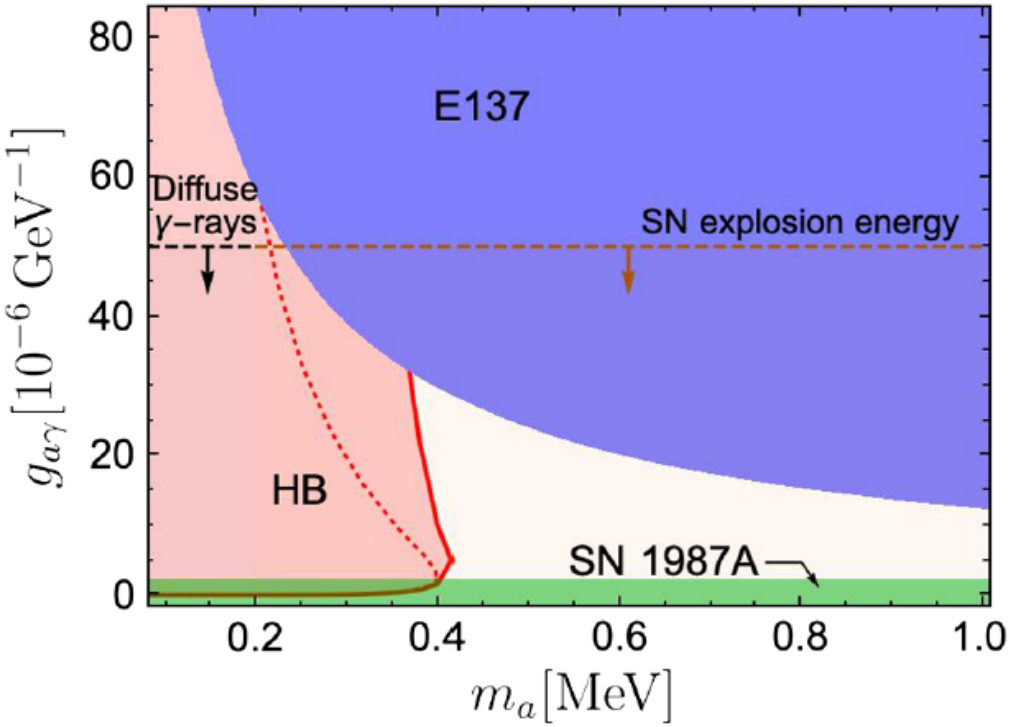

- ***Main issues: He abundance, multiple populations, poor statistics***
- ***Theoretical uncertainty:*** **semiconvection, $^{12}C(\alpha,\gamma)^{16}O$ reaction rate**
- **Possible alternatives**

The RGB tip of Globular Clusters

- The tip of the red giant branch (RGB) coincides with the thermonuclear runaway powered by the He ignition (3α) within the degenerate core of a low-mass star (typically 0.8-0.9 M$\odot$).
- The observable used to constrain the new physics is **the luminosity of the RGB tip**, which is essentially determined by the concurrent action of energy sources (nuclear burning + gravity) and energy sinks (plasma neutrinos+ bremsstrahlung axions).

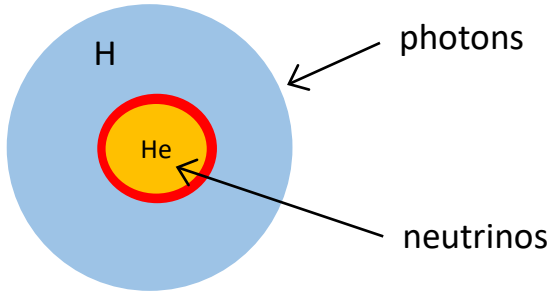

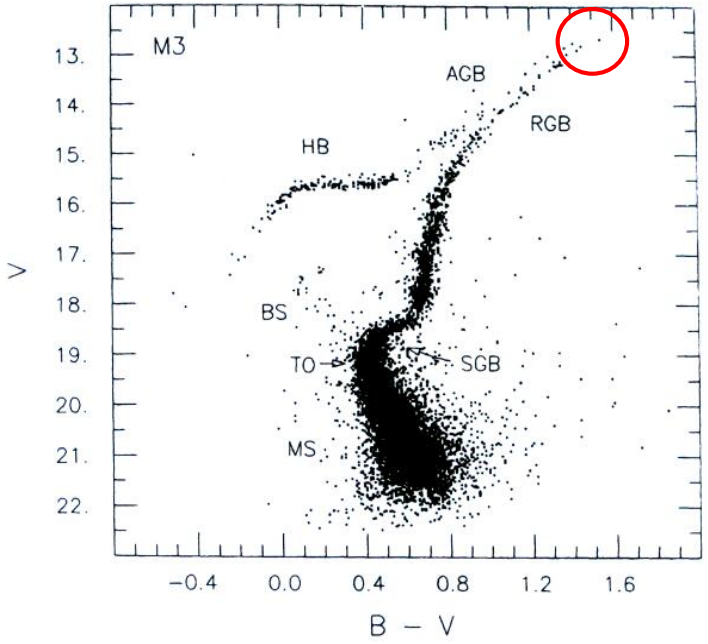

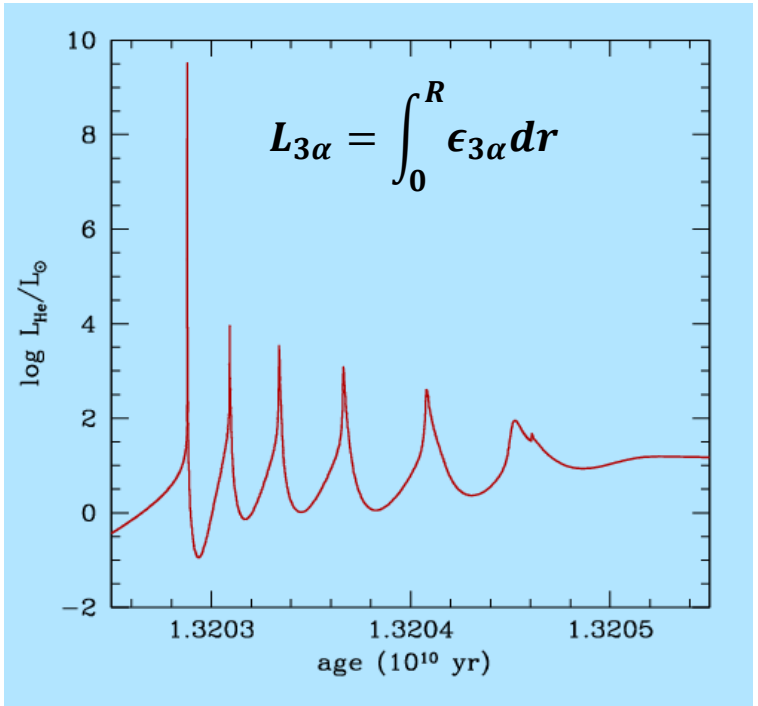

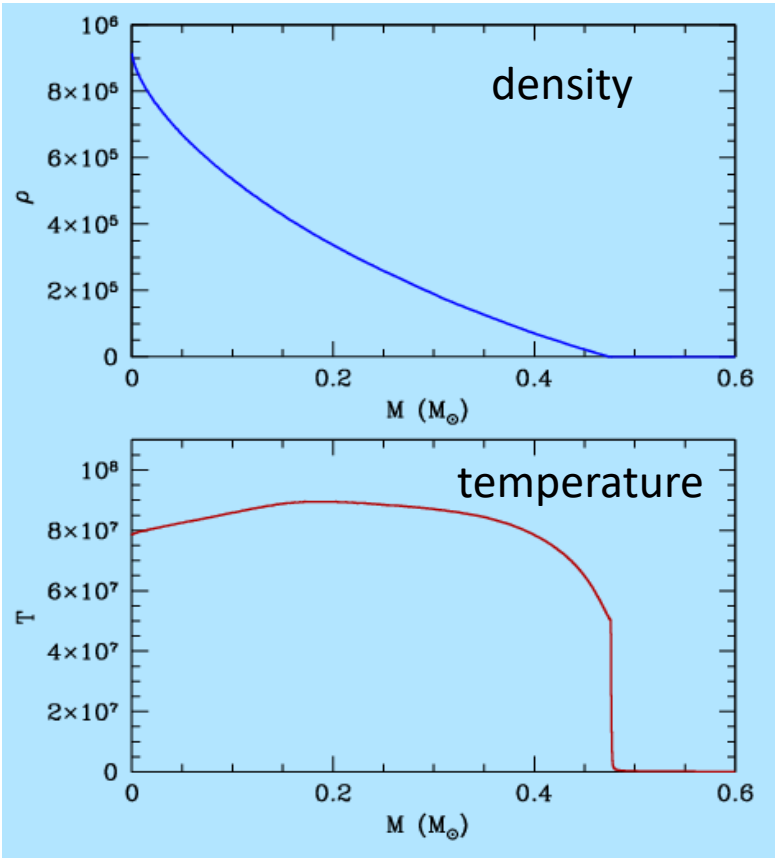

Neutrino and axion energy-loss in RGB stars

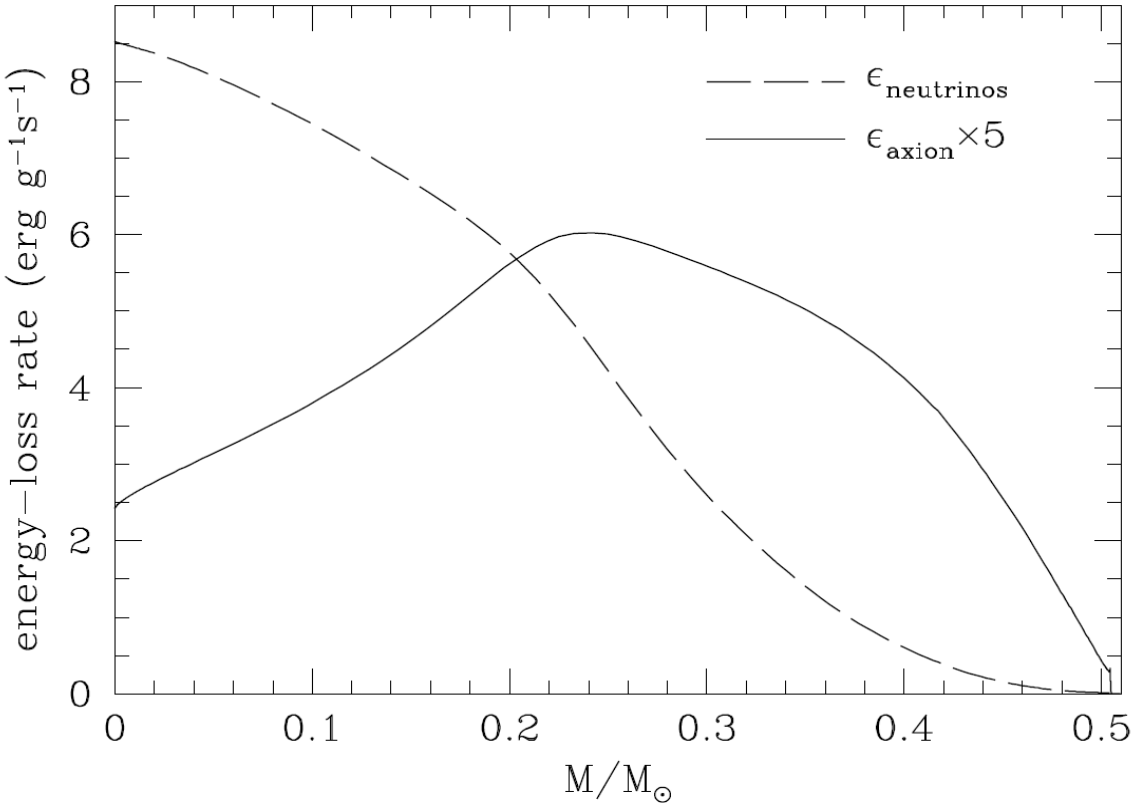

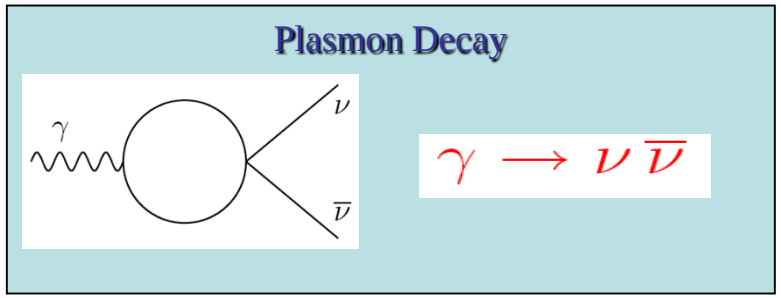

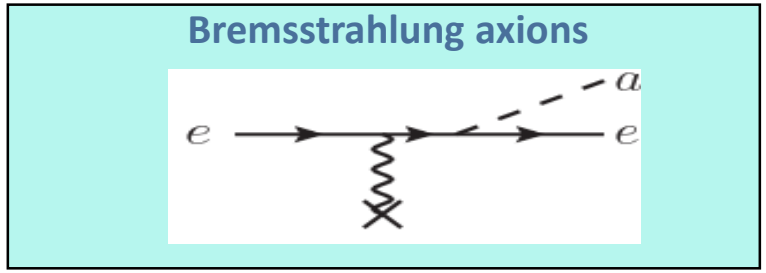

The plasma neutrino production is larger at higher density, while Bremsstrahlung axions are mainly produced round the max T layer.

g_{ae} from RGB tip luminosity

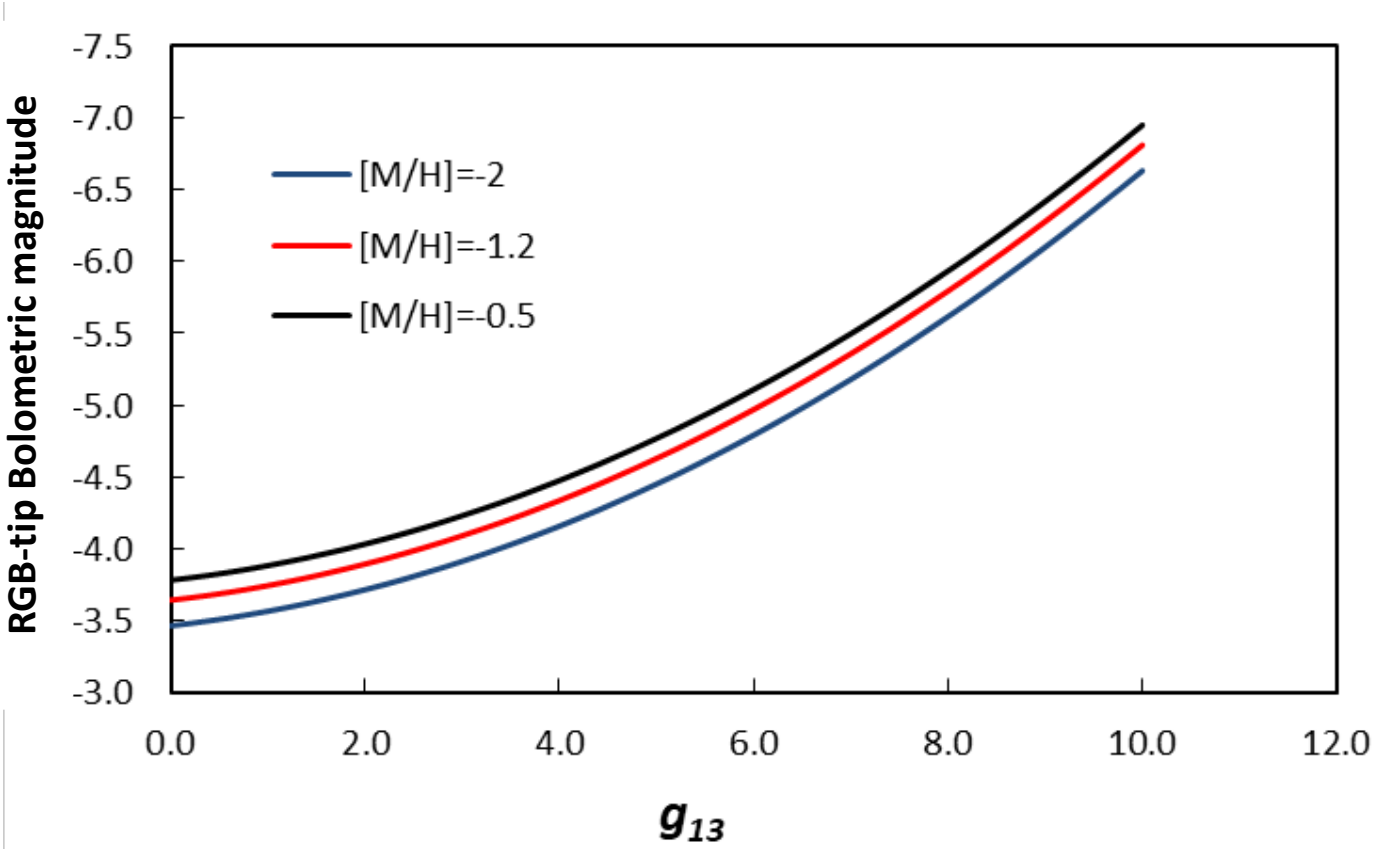

Bremsstrahlung Axions make the RGB tip brighter.

M_{bol} =4.75-2.5 log($L/L_{\odot}$) [M/H] = log(Z/X) – log$(Z/X)_{\odot}$

Theory error budget of the RGB tip luminosity (see, Straniero+ 2020).

parameter	reference	uncertainty	ΔM_{bol}[1]
η (mass loss)	Reimers	0.1 : 0.5	0.014
14N+p	STARLIB (LUNA)	±10%	0.016
3α	STARLIB (NACRE)	±20%	0.033
screning 3α	Dewitt 1973 + Graboske 1973 + Itoh 1979	±20%	0.035
neutrinos	Haft 1994 + Itoh 1996	±5%	0.026
e conductuvity	Potekin 1999	±5%	0.049
rad. opacity	OPAL+COMA 2006	±5%	< 0.001
α (mix. length)	1.82 (SSM calibrated)	1.62 : 2.02	< 0.001
boundary condition	$T(\tau)$ rel. (Krishna Swamy 1966)	±10%	< 0.001
Eq. of state	OPAL 2005 + Straniero 1988	see text	0.003
microscopic diffusion	Thoul et al. 1994	see text	0.006 to 0.025
rotation	Piersanti et al. 2013	0-100 km/s	< 0.01

[1]Full width variation of the tip bolometric magnitude.

← Larger at lower Z

Initial rotation velocity

- The last column reports the full-width variation of the RGB tip bolometric magnitude as obtained varying a single physics input.
- In principle, error correlations may be important.

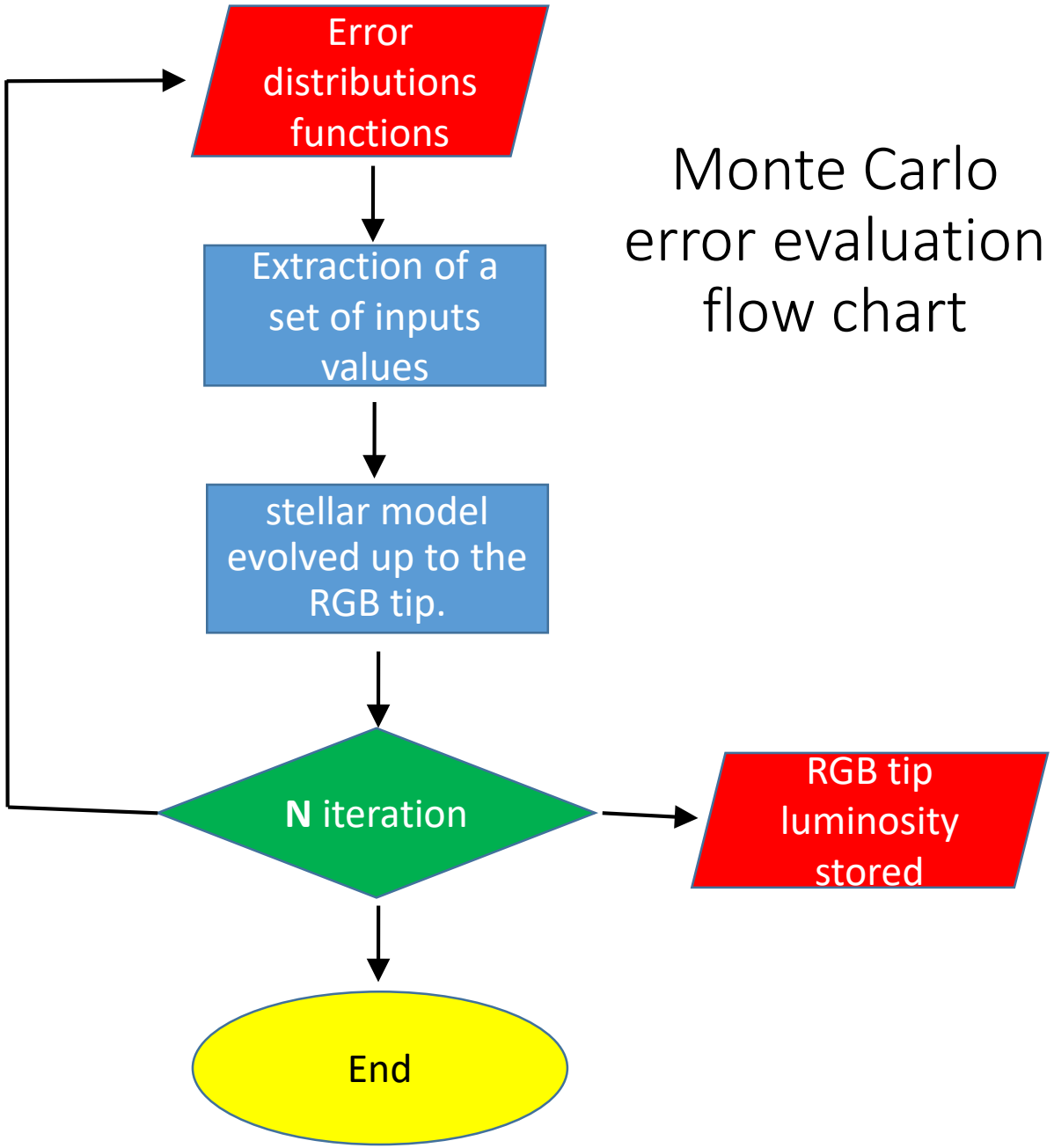

Monte Carlo error evaluation flow chart

Global theoretical error for the RGB tip luminosity

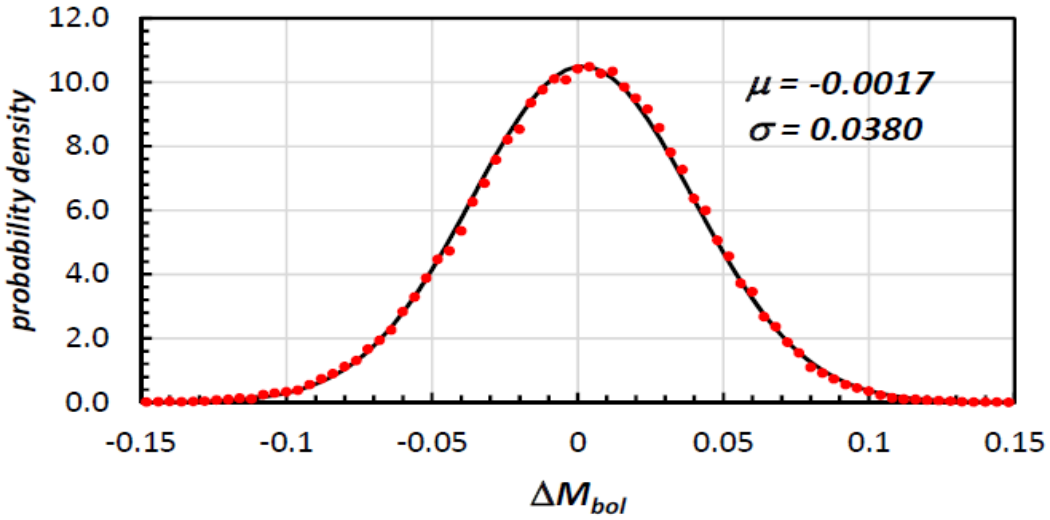

Fig. 5. Result of the Monte-Carlo error propagation: points represent the normalized frequency of Monte-Carlo events, while the curve is the best fit Gauss function. Mean and standard deviation are shown.

$$\sigma_{theory} = \pm 0.04\ mag$$

Our GC data catalog

- Parallaxes (GAIA EDR3).
  - ↳ distances.
- Proper motions and radial velocities (GAIA EDR3, HST).
  - ↳ distances & memberships.
- B,V,I,R,J,H,K magnitudes and colors (HST, VLT, 2MAS, NTT, TNG)
  - ↳ bolometric magnitude of RGB stars & distances.

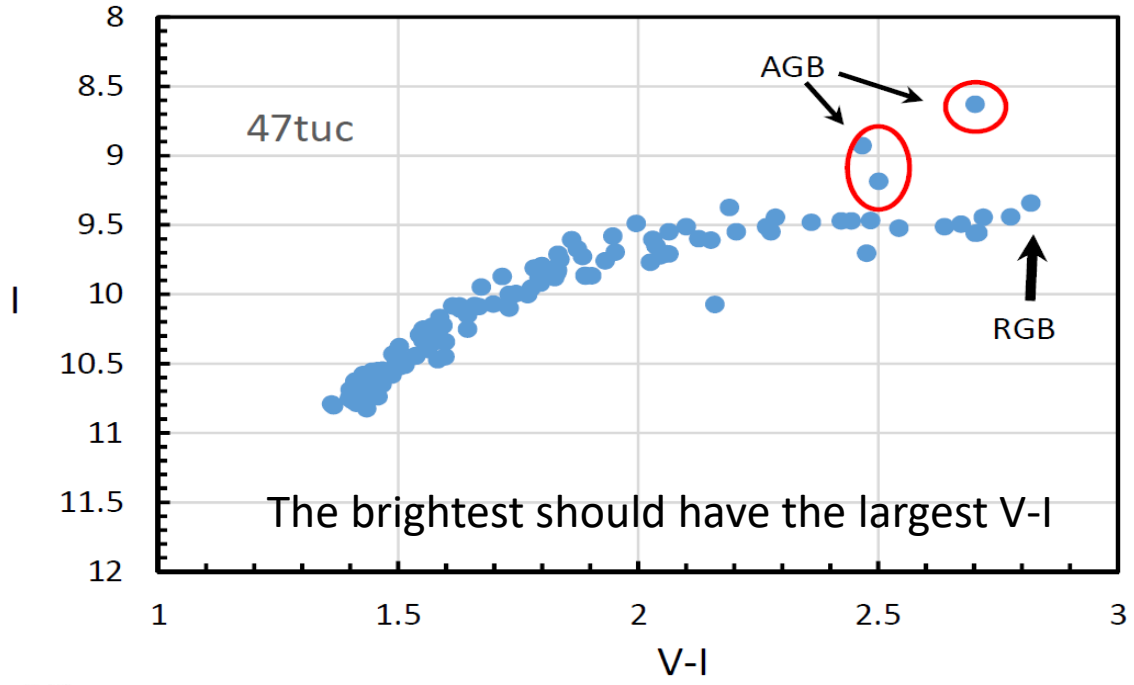

STEP1. Identification of the brightest RGB star.
Main issues: field objects and AGB stars contaminations of the RGB sample. True RGBs selected by means of colours, variability mode and proper motions (if available).

STEP2. Guess the RGB tip.
Based on synthetic CMD diagrams

N=number of stars in the brightest part (2.5 mag) of the RGB

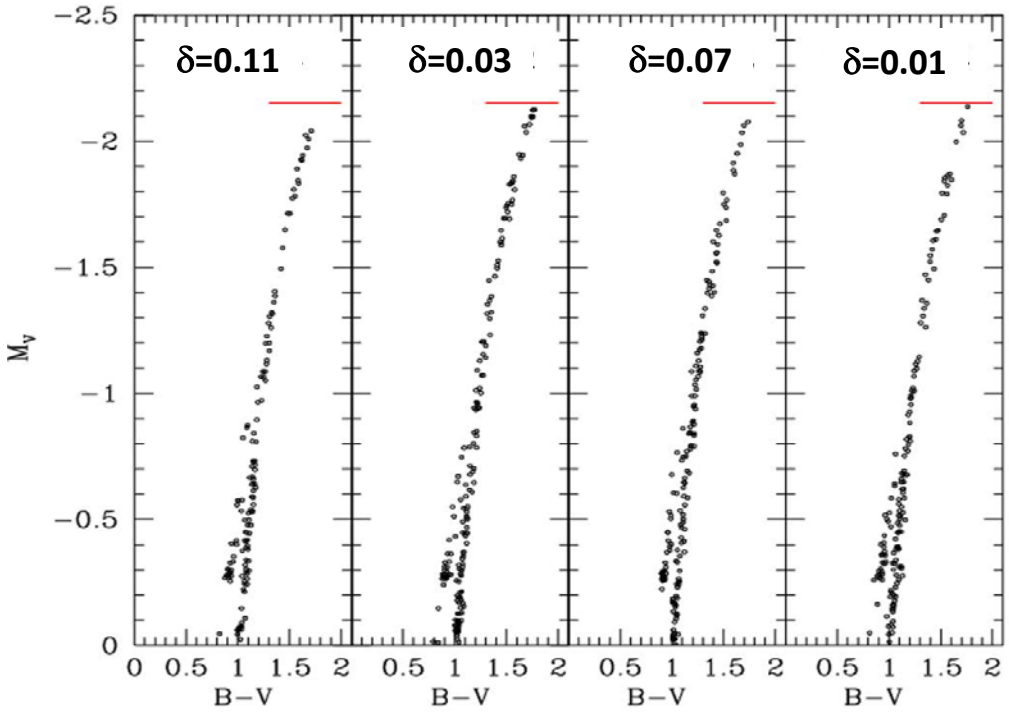

$$m_{tip} = m_{BS} - \langle\delta\rangle_N$$

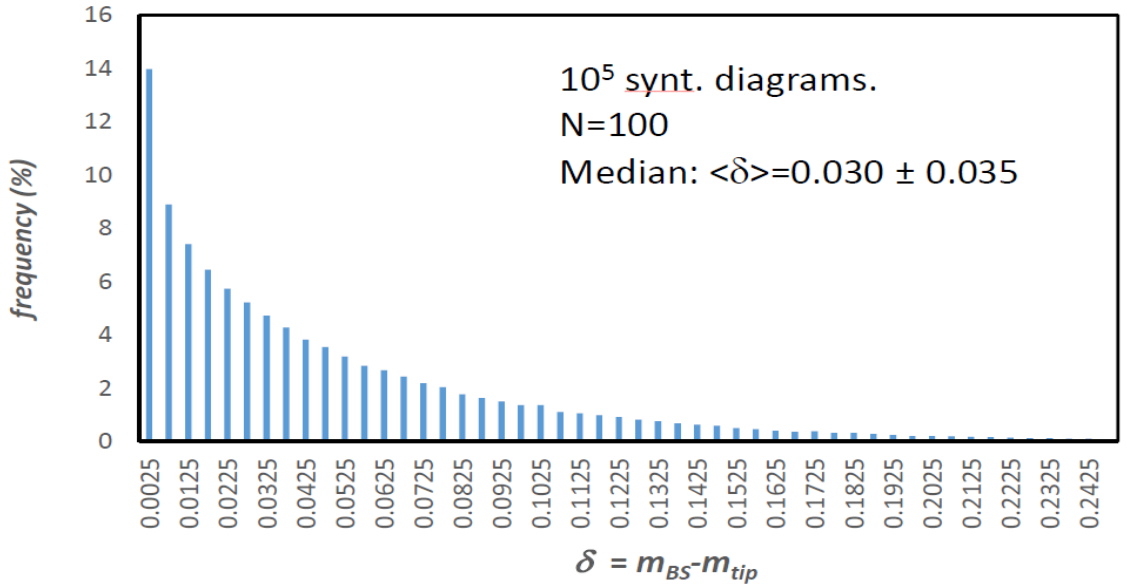

Distances: a major improvement, by combining independent determinations.

- Parallaxes (GAIA EDR3)
- Kinematic (GAIA EDR3, HST)
- Subdwarf main-sequence fitting (HST and ground-based photometry)
- ZAHB fitting (HST and ground-based photometry)
- RR Lyrae P-L relation
- Eclipsing binaries
- Other methods (if available)

One may adopt a mean value, which maximize the likelihood; This method may also shed light on hidden systematic errors.

Results: 21 Clusters with improved distances:

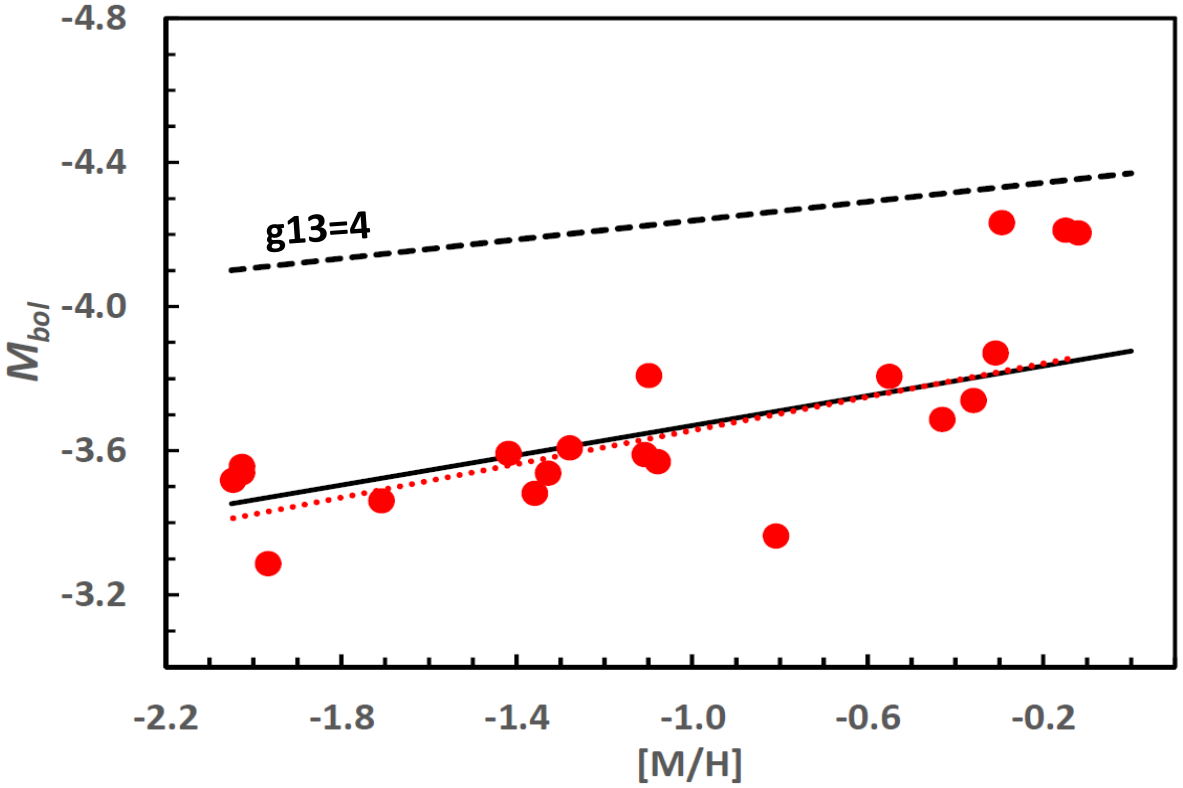

g_{ae} = 0 (black-solid line) and g_{ae} = 4 10^{-13}(black-dashed line). The red-dotted line represents the least square fit of the 21 observed bolometric magnitude.

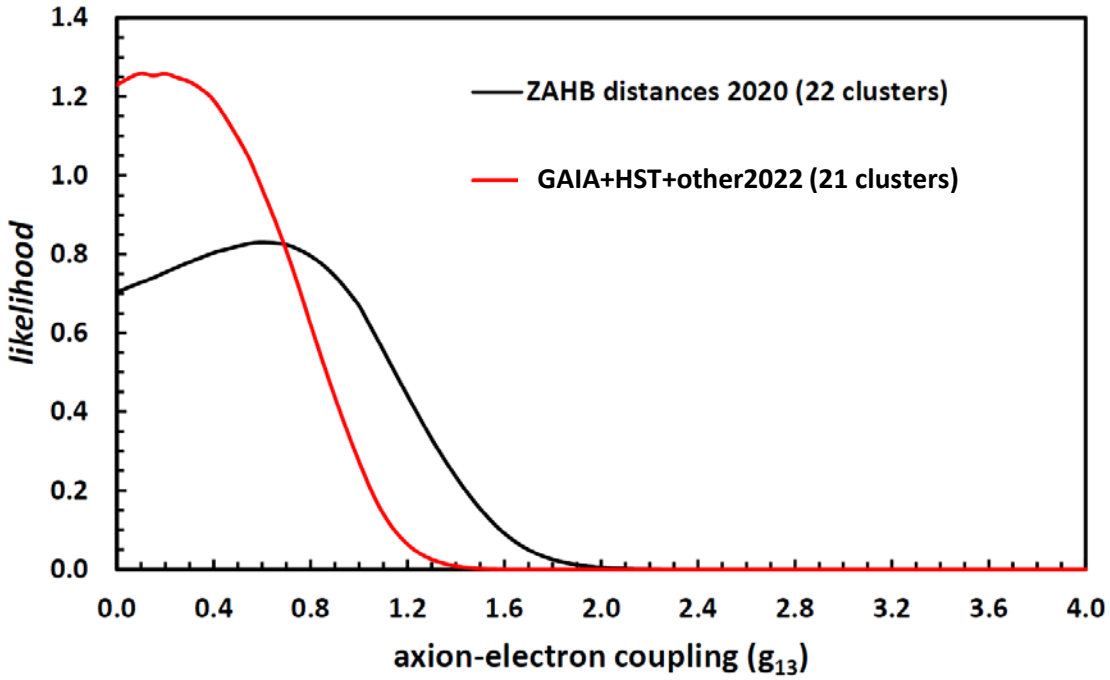

Result:

hint 68%: $g_{ae}/10^{-13} = 0.10^{+0.22}_{-0.10}$

bound 95%: $g_{ae}/10^{-13} < 0.96$

the most stringent bound for the axion-electron coupling.

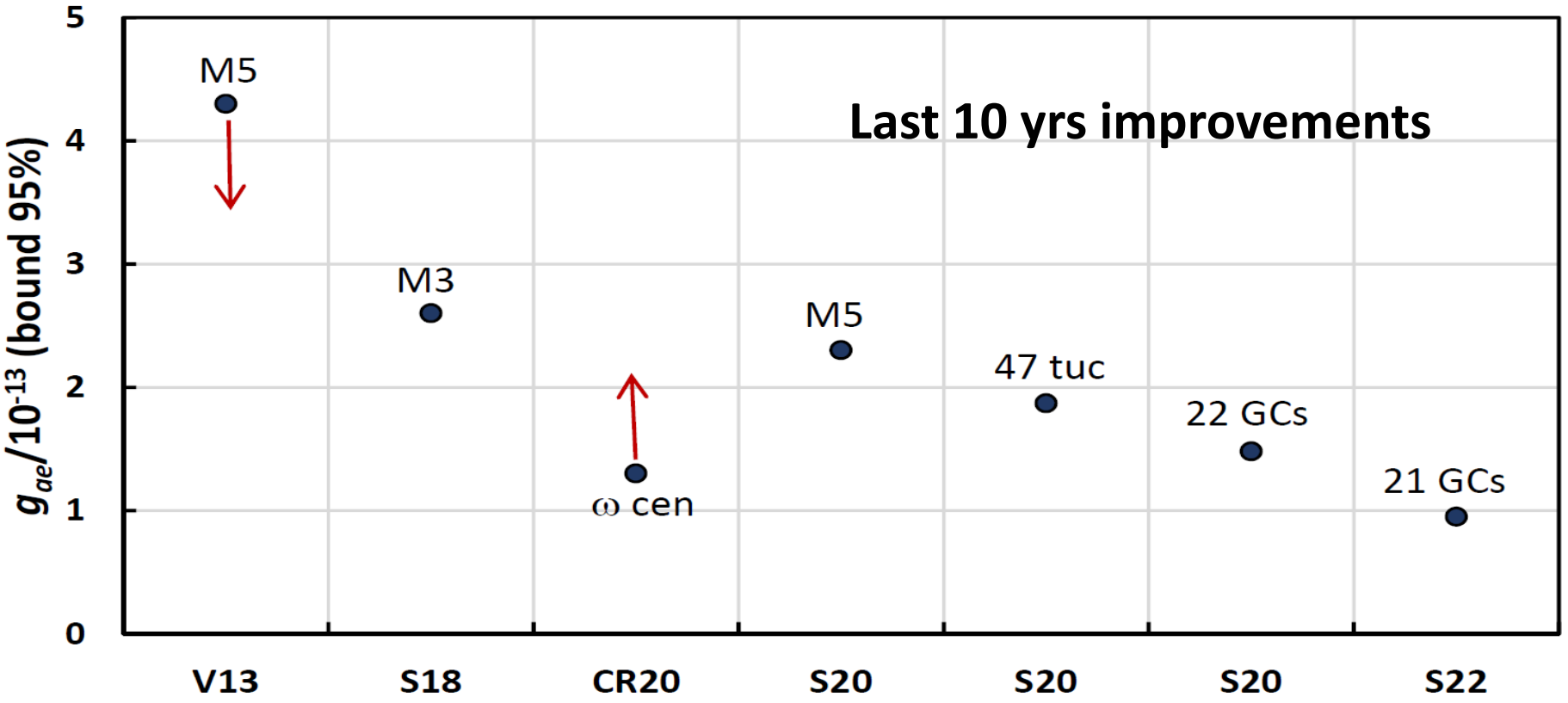

V13=Viaux+ 2013 - S18=Straniero+ 2018 – CR20=Capozzi & Raffelt 2020 – S20= Straniero+ 2020 – S22=present work

Some Remarks:

- V13 underestimate L_{tip} theory, because of the weak 3α screening (no ion-electron couplings).
- CR20 underestimate the ω Cen distance (kinematic), because of the ellipticity of this cluster.
- S20, for 47 tuc use distance from GAIA DR2 parallax. For the others, use ZAHB normalized to 47 tuc.
- S22 revised distances after GAIA DR3 .

SENSITIVITY OF VARIOUS EXPERIMENTS & GC BOUNDS

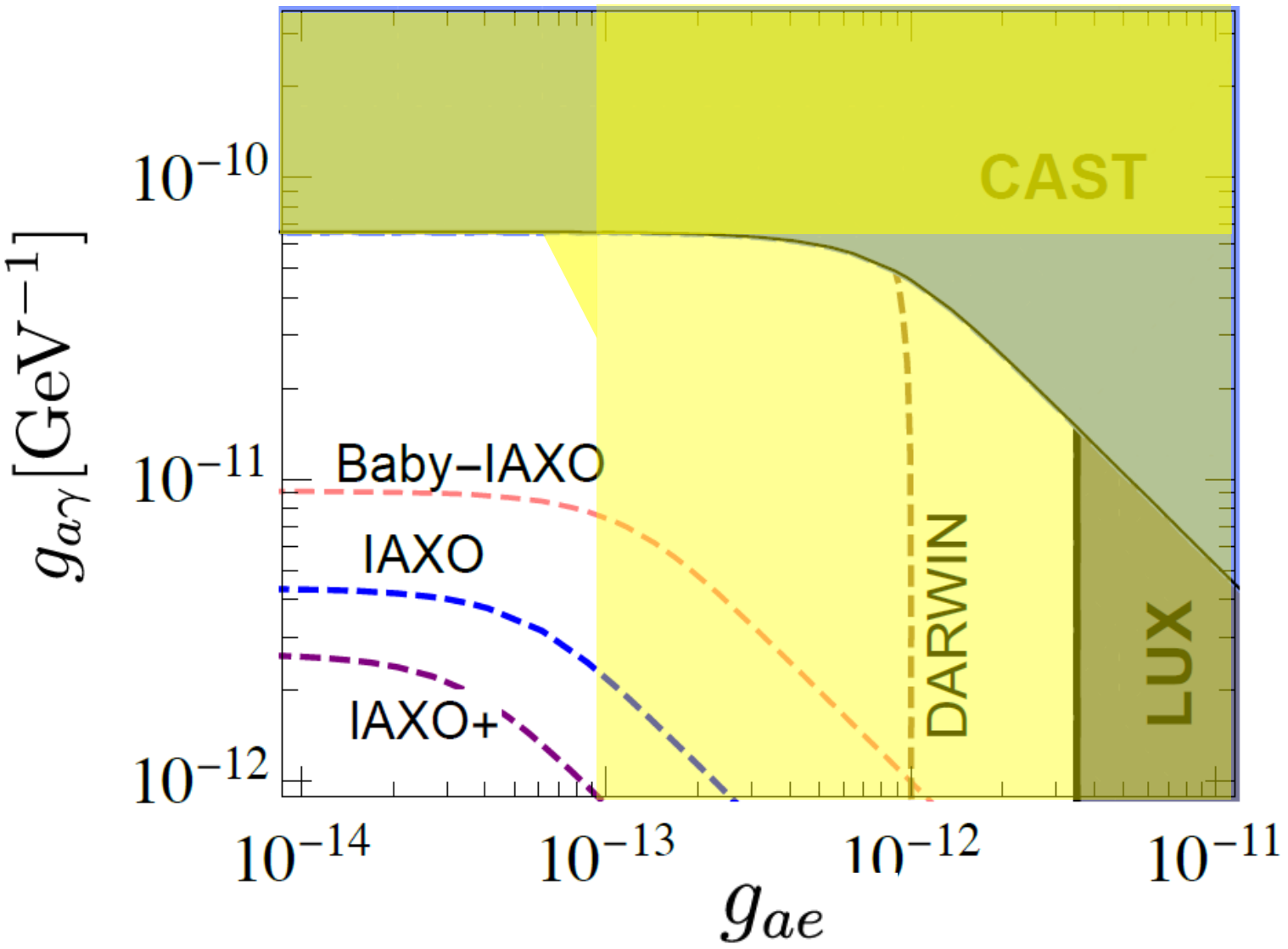

Yellow areas delimit the regions which are excluded by RGB and HB stars (RGB tip luminosity and *R* parameter) bounds.

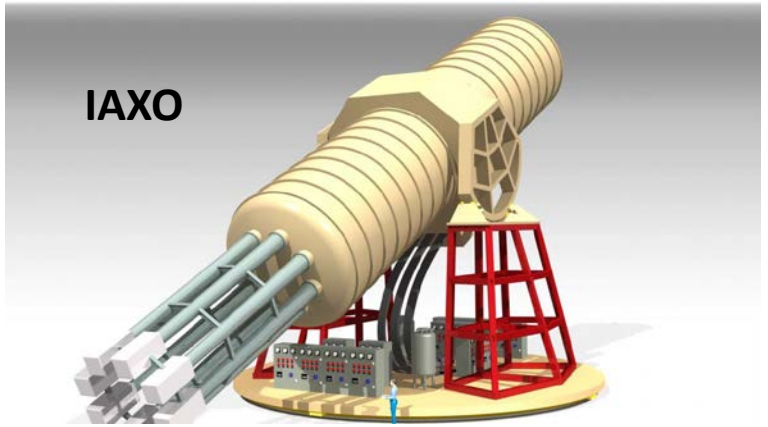

The advanced phases of massive stars evolution

A STAR EVOLVES also BECAUSE IT LOSES ENERGY. Till the core-He burning, the energy loss is mainly due to the radiation emitted from the stellar photosphere. However, during the C burning and beyond , the evolution of massive stars is controlled by the thermal neutrino production. Thermal processes can also release ALPs. The **red point** marks the beginning of the C burning. The expected ALP luminosity substantially increase as stars approache the final core collapse.

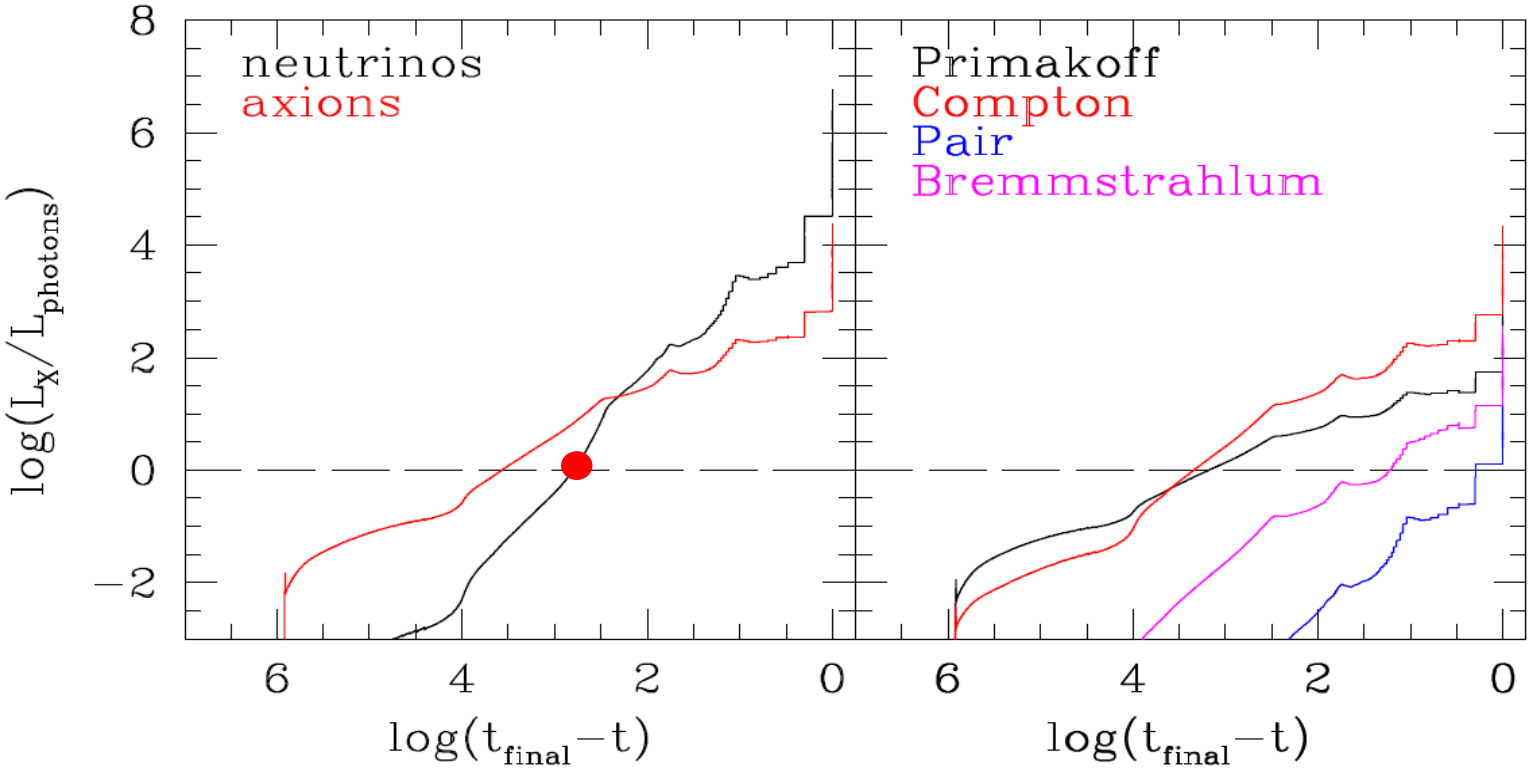

For a small sample of type II SNe, the progenitors have been discovered in pre-explosive photometric frames.

from Smartt 2015

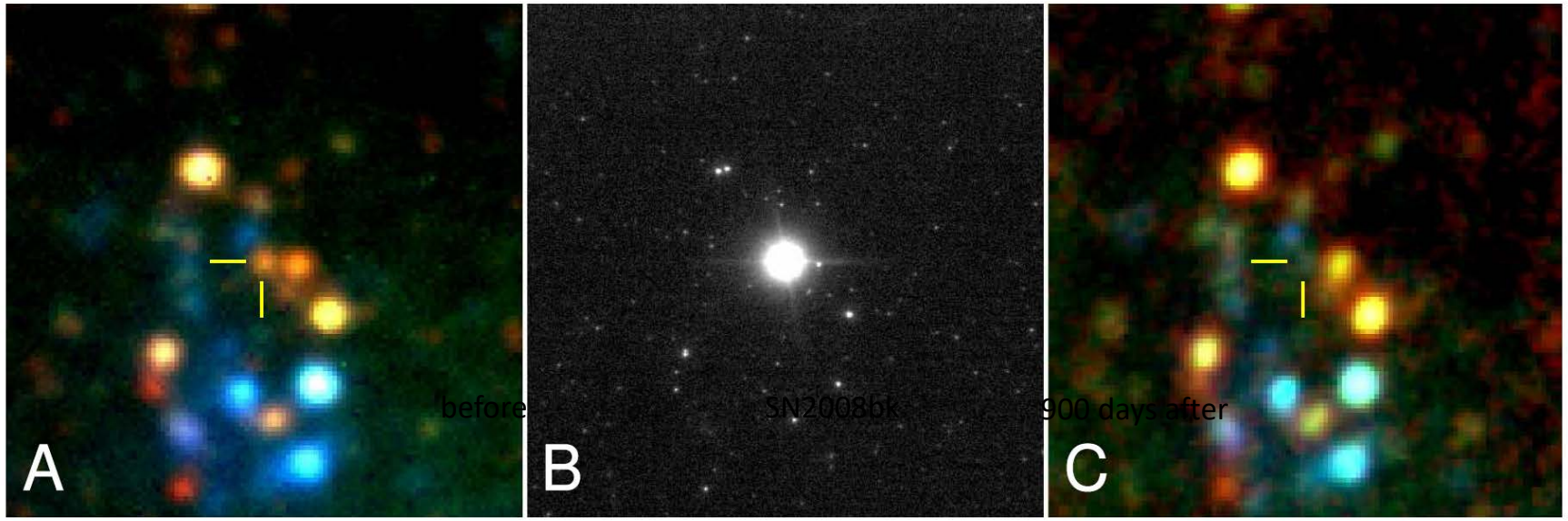

Figure 8. Upper: The visually striking illustration of the disappearance of the red supergiant progenitor of SN2008bk, from Mattila et al. (2010). Panel A shows the VLT colour image of the progenitor (marked). Panel B shows the VLT NACO image of SN2008bk and the surrounding population at high resolution. Panel C shows an NTT colour image at approximately 940 days after explosion illustrating the disappearance of the red source. The quantitative mass estimates of the progenitor are in Maund et al. (2014a).

The luminosity of SN progenitors

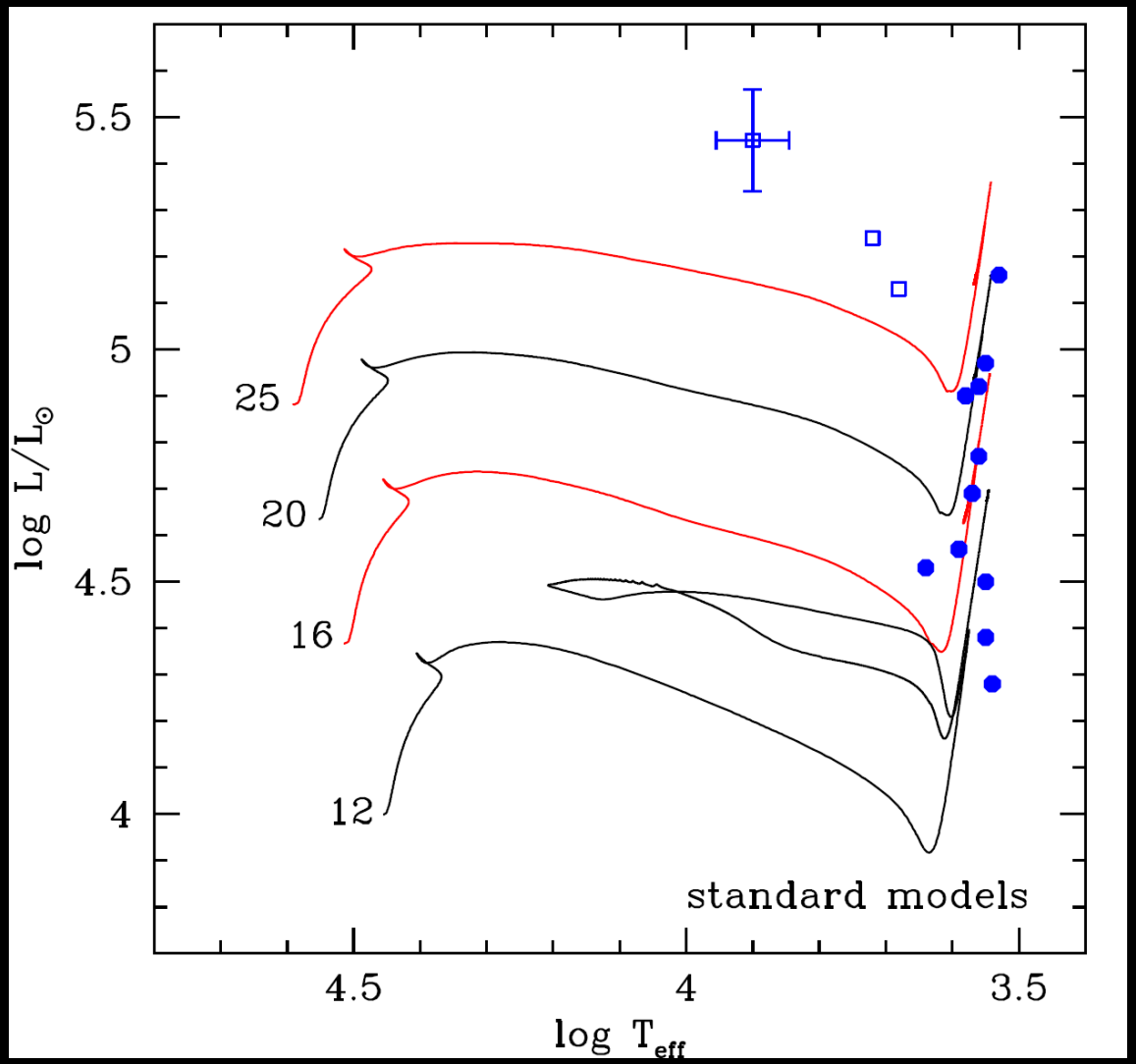

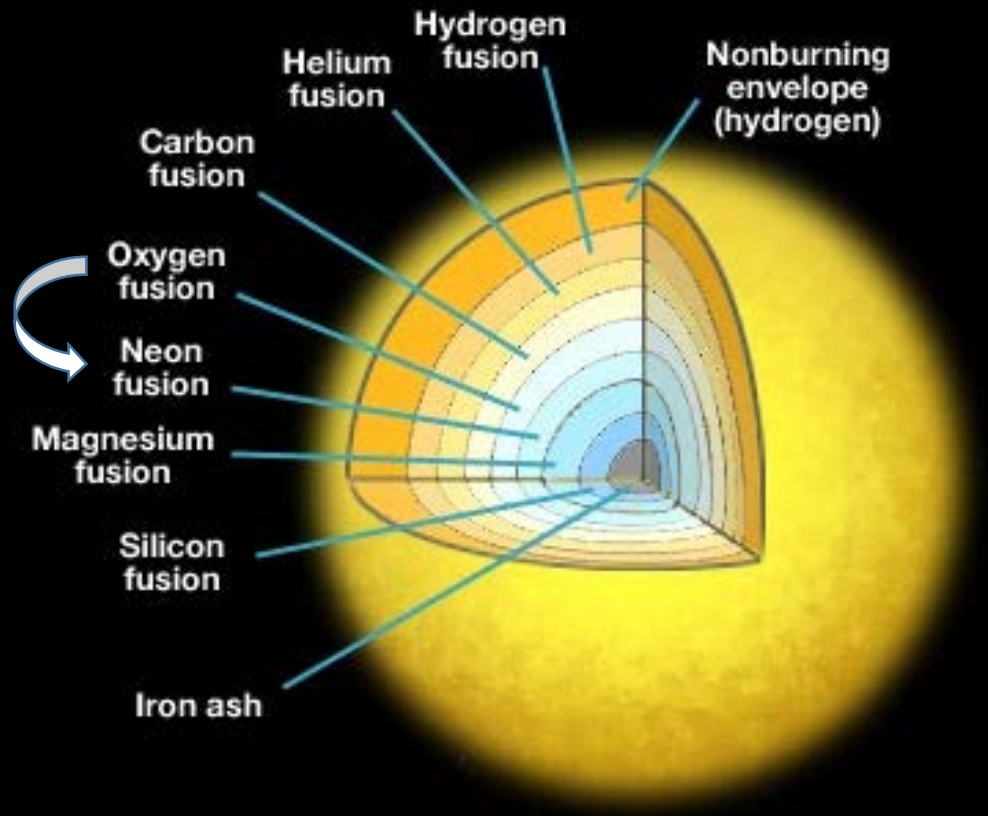

Blue points represent Red Supergiant progenitors of type IIP SNe.
From Straniero et al. 2019, ApJ 881, 158

The luminosity at the core collapse is lower in case of axions

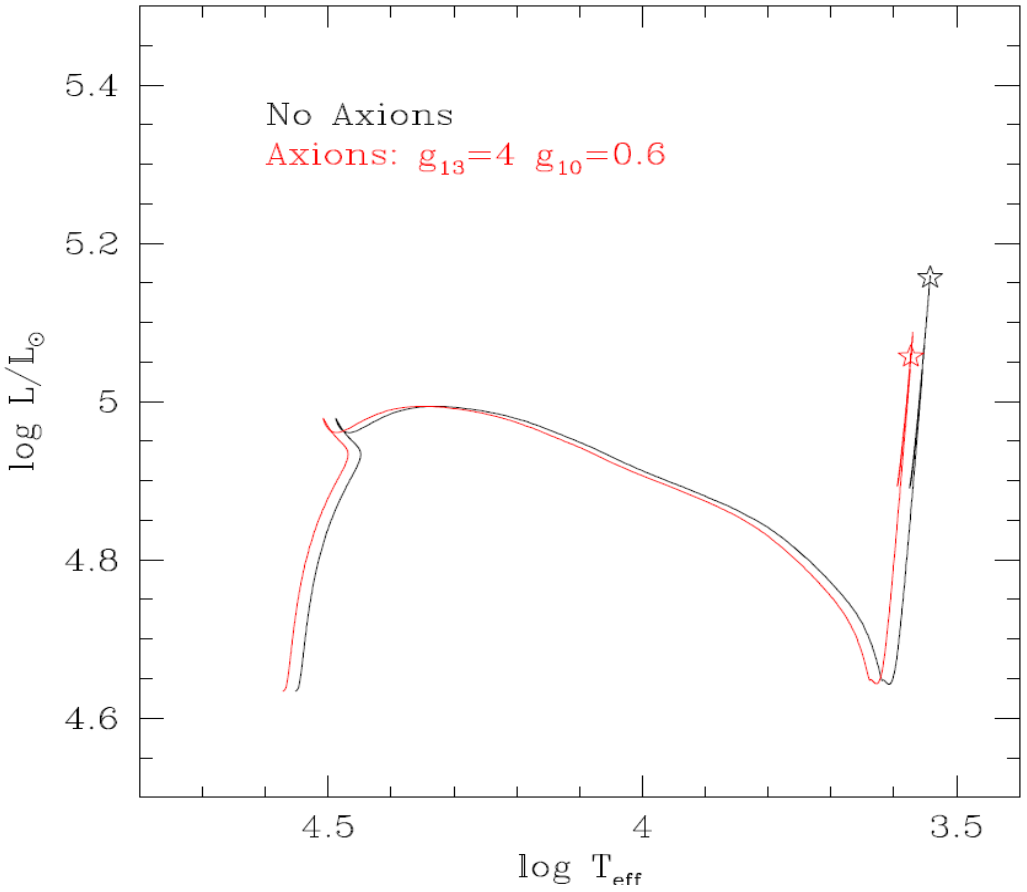

Evolutionary tracks of non-rotating 20 Mʘ models with and without axion cooling (Straniero+ 2019)

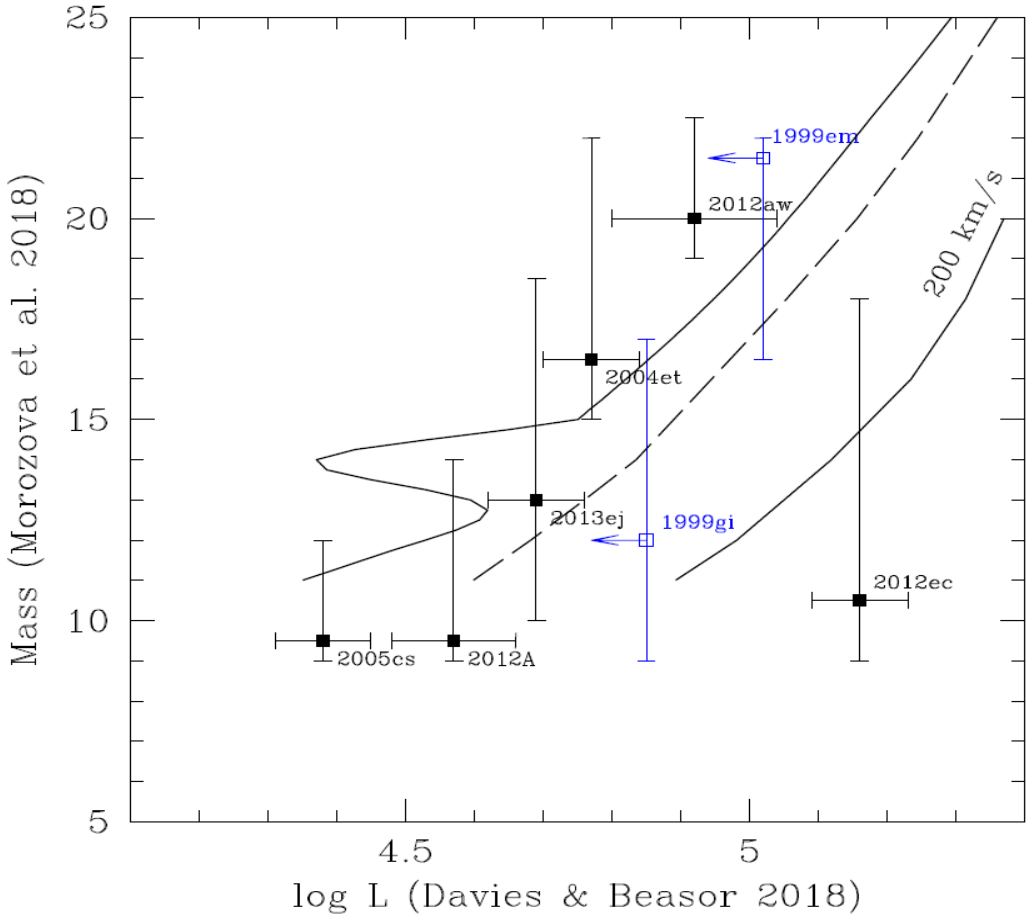

Initial mass-final luminosity relation: solid lines represent models with axions, the brightest also with rotation (200 Km/s initial v). Dashed line represents no-axion models (no-rotating)

The X-ray signature of axion production in Core-collapse Supernova progenitors.

Once emitted, ALPs can be converted into photons (X-tays) when traveling within the galactic magnetic field. The signature of this phenomenon can be searched in the X-ray spectra of galactic supergiants.

TABLE I. Models of ALP production from Betelgeuse. The stage of stellar evolution is parametrized by the time remaining until the core collapse for Betelgeuse, t_{cc}. See text for the definition of other parameters.

					Primakoff			Bremsstrahlung			Compton		
Model	Phase	t_{cc} [yr]	$\log_{10}\frac{L_{eff}}{L_\odot}$	$\log_{10}\frac{T_{eff}}{K}$	C^P	E_0^P [keV]	β^P	C^B	E_0^B [keV]	β^B	C^C	E_0^C [keV]	β^C
0	He burning	155000	4.90	3.572	1.36	50	1.95	1.3×10^{-3}	35.26	1.16	1.39	77.86	3.15
1	Before C burning	23000	5.06	3.552	4.0	80	2.0	2.3×10^{-2}	56.57	1.16	8.55	125.8	3.12
2	Before C burning	13000	5.06	3.552	5.2	99	2.0	6.4×10^{-2}	70.77	1.09	17.39	156.9	3.09
3	Before C burning	10000	5.09	3.549	5.7	110	2.0	8.9×10^{-2}	76.65	1.08	22.49	169.2	3.09
4	Before C burning	6900	5.12	3.546	6.5	120	2.0	0.136	85.15	1.06	31.81	186.4	3.09
5	In C burning	3700	5.14	3.544	7.9	130	2.0	0.249	97.44	1.04	50.62	210.4	3.11
6	In C burning	730	5.16	3.542	12	170	2.0	0.827	129.17	1.02	138.6	269.1	3.17
7	In C burning	480	5.16	3.542	13	180	2.0	0.789	134.54	1.02	153.2	279.9	3.15
8	In C burning	110	5.16	3.542	16	210	2.0	1.79	151.46	1.02	252.7	316.8	3.17
9	In C burning	34	5.16	3.542	21	240	2.0	2.82	181.74	1.00	447.5	363.3	3.22
10	Between C/Ne burning	7.2	5.16	3.542	28	280	2.0	3.77	207.84	0.99	729.2	415.7	3.23
11	In Ne burning	3.6	5.16	3.542	26	320	1.8	3.86	224.45	0.98	856.4	481.2	3.11

TOOLS and Method

see Mengjiao Xiao+ 2020 and 2022

The expected photon flux from a nearby massive star is :

$$\frac{dN_\gamma}{dEdSdt} = \frac{1}{4\pi d^2}\frac{d\dot{N}_a}{dE}P_{a\gamma}.$$

where B_T is the transverse magnetic field, q is the momentum transfer, and d is the magnetic field length.

The ALP-photon conversion probability is [41]

$$P_{a\gamma} = 8.7 \times 10^{-6} g_{11}^2 \left(\frac{B_T}{1\ \mu\text{G}}\right)^2 \left(\frac{d}{197\ \text{pc}}\right)^2 \frac{\sin^2 q}{q^2},$$

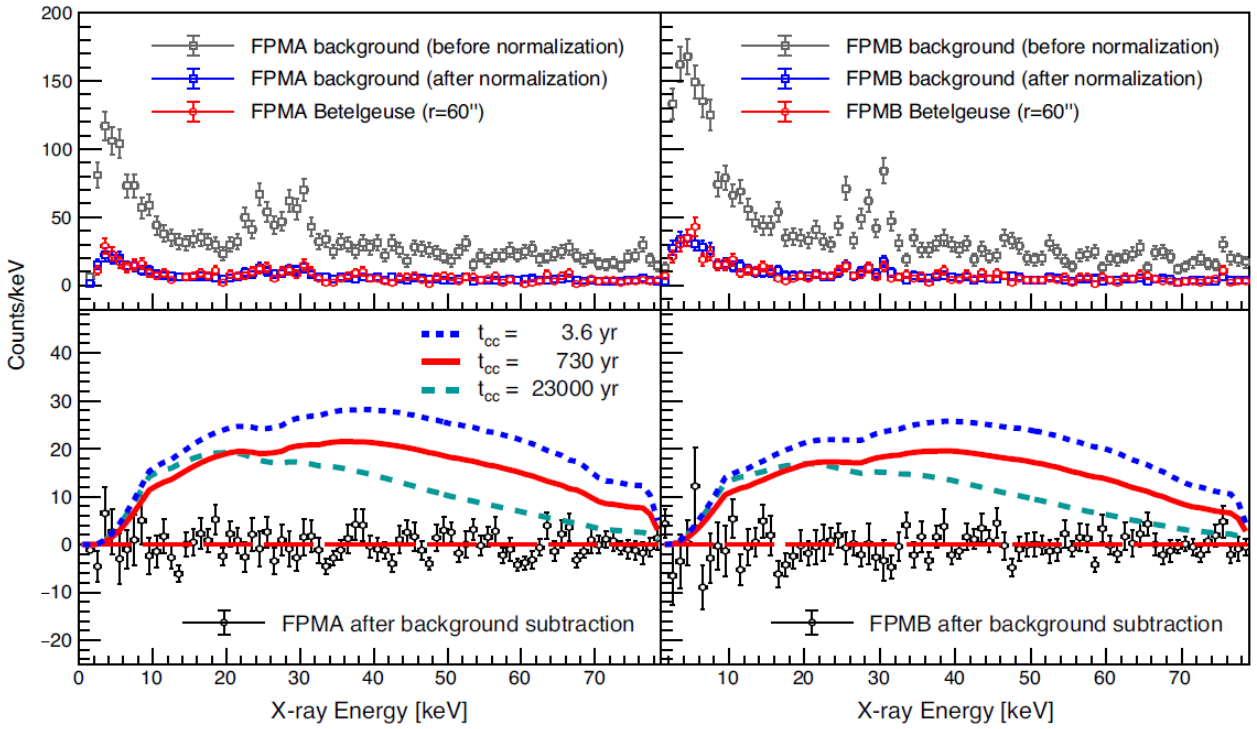

- Top: X-ray spectra from NuSTAR for the Betelgeuse source (red) and background (gray and blue)
- Bottom: Source spectra after subtracting the normalized background. The predicted ALP-produced x-ray spectra assuming B_T = 1.4 μG, mass $m_a = 10^{-11}$ eV, and coupling $g_{a\gamma} = 1.5 \times 10^{-11}$ GeV−1.

RESULTS

Since the end of the He burning to the final core collapse, the stellar luminosity and the effective temperature do not change significantly. So, we do not know in which phase is currently Betelgeuse.

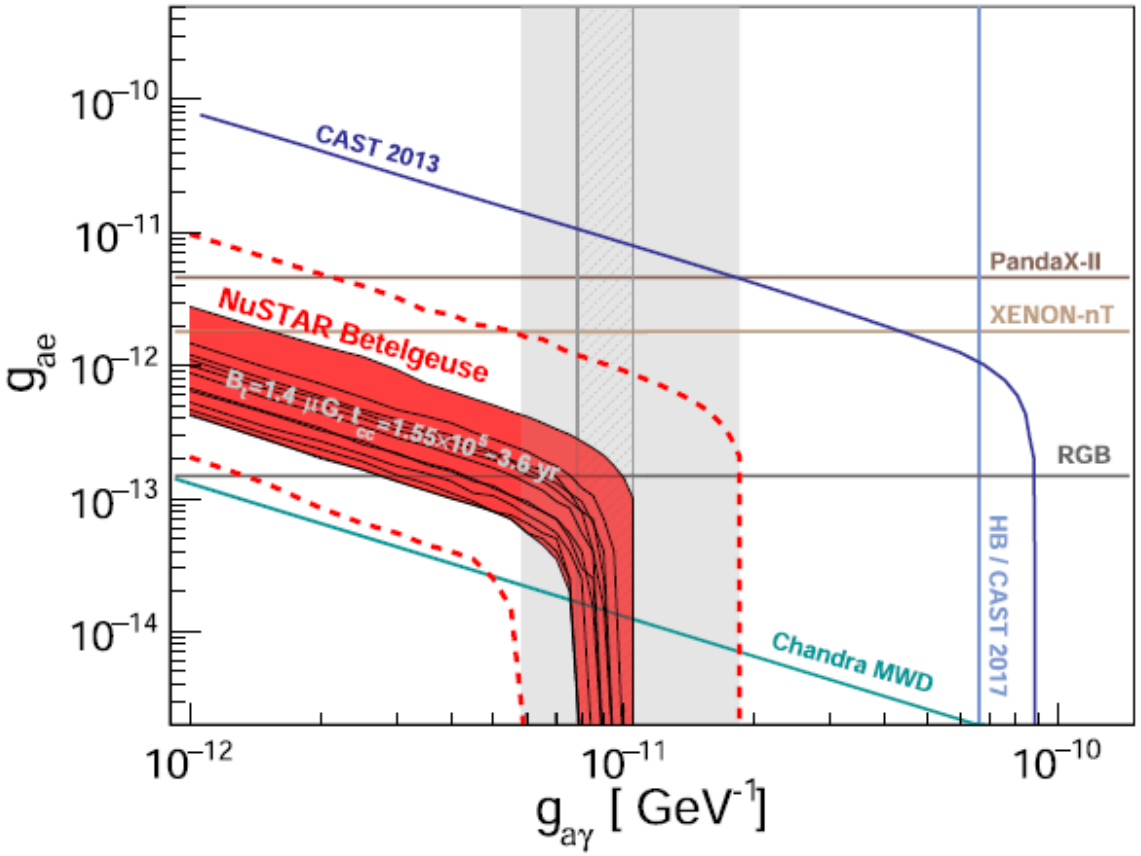

On the other hand, the central temperature and, in turn, the axion luminosity significantly increase approaching the core collapse.

For $m_a \leq 3.5 \times 10^{-11}$ eV and a reguuar Galactic magnetic field in the direction transverse to Betelgeuse B_T = 1.4 μG, we find:

$g_{a\gamma} \times g_{ae} < 2.8 \times 10^{-24}$ GeV^{-1} (in case Betelgeuse is a He-burning star)

$g_{a\gamma} \times g_{ae} < 4 \times 10^{-25}$ GeV^{-1} (in case Betelgeuse is a Ne-burning star)

Need to extend the measure to other Galactic red supergiants.

Concluding Remarks

- Stars are a natural laboratory to test new physics theories.
- Evolved stars in Globular Clusters constitute a large stellar sample to successfully carry on such kind of studies.
- White dwarfs cooling rates and luminosity functions are other important observables that allow us to constrain axions or other feebly interactive particles (see the extensive work by J. Isern & co) .
- The Sun and Supergiants close to the final core collapse are potential targets for a direct detection of axions.
- LSST may substantially improve the sample of galactic WDs and supergiant stars. The high angular resolution of near IR observation with JWST may improve GCs constraints.

More plots

$R2=N_{AGB}/N_H$

B	***R2***
Sandquist 00	0.148±0.007
Piotto 02	0.121±0.006
Sarajadini 07	0.127±0.005
Costantino 16	0.117±0.005